EPITAXIC SUBLIMATION METHODS FOR THE STUDY OF PSEUDO-BINARY SEMICONDUCTOR ALLOYS

Jay N. Zemel

Pennsylvania University

Prepared for:

Naval Ordnance Laboratory
Advanced Research Projects Agency

15 September 1972

PROGRESS REPORT

"EPITAXIC SUBLIMATION METHODS FOR THE STUDY OF PSEUDO-BINARY SEMICONDUCTOR ALLOYS"

FOR THE PERIOD 1 JUNE 1971 - 31 MAY 1972

CONTRACT N60921-70-C-0251

U.S. NAVAL ORDNANCE LABORATORY

WHITE OAK

SILVER SPRING, MARYLAND

LABORATORY FOR RESEARCH ON THE STRUCTURE OF MATTER

UNIVERSITY of PENNSYLVANIA

PHILADELPHIA, PENNSYLVANIA 19104

APPROVED FOR PUBLIC RELEASE;
DISTRIBUTION UNLIMITED

47

LABORATORY FOR RESEARCH ON THE STRUCTURE OF MATTER

UNIVERSITY OF PENNSYLVANIA

PHILADELPHIA, PENNSYLVANIA 19104

PROGRESS REPORT
"EPITAXIC SUBLIMATION METHODS FOR THE STUDY OF PSEUDO-BINARY SEMICONDUCTOR ALLOYS"

FOR THE PERIOD 1 JUNE 1971 - 31 MAY 1972

CONTRACT N60921-70-C-0251

U.S. NAVAL ORDNANCE LABORATORY

WHITE OAK

SILVER SPRING, MARYLAND

Sponsored by

ADVANCED RESEARCH PROJECTS AGENCY

ARPA Order No. 1597

Jay N. Zemel
Principal Investigator
University of Pennsylvania

Donald N. Langenberg
Director
Laboratory for Research
on the Structure of Matter

DATE: 15 September 1972

PROGRESS REPORT

(Twelve Months)

1 June 1971 – 31 May 1972

INTRODUCTION

During the past years, research on the pseudobinary alloys has rapidly grown out of the initiating stage and into a fully productive phase. The "parting layer" and the "hot wall" techniques of epitaxic film growth have been extensively and successfully tested and are now in operation. The research on the PbO_xS_{1-x} has been extended to photoconductivity measurements, indicating a significant enhancement of photoconductivity as a result of introduction of oxygen. Use of modulation spectroscopy techniques for the study of the optical properties of the films was initiated and extensive thermoreflectance measurements were carried out on the IV-VI compounds and the resulting structures were identified with the critical points in their energy band structure. The surface wave studies have progressed with generation of 200 MHz Rayleigh waves using transducers of aluminum interdigital arrays on quartz. The experimental system for the physiochemical studies of PbS-PbO system was completed and a large number of kinetic studies were carried out.

In the theoretical area, a full-relativistic APW program based on the Dirac's equation has been developed and successfully

tested on SnTe. The calculation of the deformation potential for the L extrema of the lead chalcogenides and SnTe was completed.

The formal interaction with the Naval Ordnance Laboratory within this project and the informal interaction with the Physics Department and the School of Metallurgy and Materials Science of the University of Pennsylvania has been successfully continuing. On 24-25 March 1972, a Topical Conference of the American Physical Society on the Physics of IV-VI Compounds and Alloys was held at the University of Pennsylvania and sponsored by The Moore School of Electrical Engineering and the Laboratory for Research on the Structure of Matter.

EXPERIMENTAL FILM PROGRAM

1. $Pb_{1-x}Cd_xS$, PbS and PbSe

a) Growth; Parting Layer Technique. The problem of thermal expansion coefficient mismatch between alkali halide substrates and epitaxic IV-VI compounds grown on these substrates has been known for sometime. In the past few years, there has been increasing attention paid to matching of the expansion coefficients by using CaF_2 and BaF_2 which has lead to the marked improvement in the low temperature electrical properties of PbTe and $Pb_{1-x}Sn_xTe$ epitaxic films.[1]

We began with a bulk crystal of PbS, cleaved to form a regular parallelipiped. In our case, the crystal was a piece of natural galena. The apparatus used for the film deposition was similar

to that used by Bis et al.[2] for growing alloy films of the lead salts using two sources isolated from each other by a water cooled jacket (see Ref. 2). The two sources were used for evaporating NaCl and PbS onto the galena substrate. The substrate temperature was about 275°C. A layer of NaCl was deposited on PbS using identically the same procedure employed by Schoolar and Zemel[3] for the deposition of PbS on NaCl. Then the chamber was let up to atmospheric pressure for a couple of hours to allow the NaCl to be exposed to atmospheric moisture. There is some indication that this procedure assists epitaxy. Typical operating conditions are listed in Table I.

TABLE I

Substrate (Galena) Temperature	275°C
NaCl-Source Temperature	675°C
PbS-Source Temperature	700°C
Deposition Rate of NaCl	40Å/minute
Deposition Rate of PbS	40Å/minute
Thickness of NaCl Layer	0.5-1.0 μ
Thickness of PbS Layer	1μ-7μ

The thermal mismatch between NaCl and PbS is approximately 2×10^{-5}. When PbS films are grown on NaCl substrates, a strain of 0.4% in the PbS film must be relieved by plastic deformation of either the NaCl substrate or the film itself. It is not a trivial matter to relieve such a large strain and some of the lifetime problems found by

various investigators may result from this strain relief.[4] The use of a parting layer of NaCl on a PbS substrate causes the strain to occur in the NaCl layer (Fig. 1). The subsequent overgrowth of PbS should not be subjected to any thermal mismatch strain upon cooling.

The PbS films grown had thicknesses ranging from 1μ to 7μ. There does not seem to be any inherent limitations on the growth of very thick epitaxic films using this method. The PbS films were removed from the substrate by immersion in H_2O. The NaCl layer dissolved, thereby freeing the PbS film from the galena substrate. The PbS substrate showed no sign of clouding or secondary crystal growth and could be used again for further deposition after drying.

The PbS films deposited under these conditions were examined for their single crystal nature using Bragg and Laue x-ray diffraction measurements. Figure 2 shows the Bragg diffractometer recording for (600) planes of PbS film. The doublet showing reasonably good single crystal behaviour.

A rough measurement of the electrical properties was undertaken. The film was transferred to a glass slide using an optical cement. The parting layer was dissolved in water separating the substrate from the film which was firmly attached to the glass slide. The measurement indicated that mobility at room temperature was 80 cm^2/volt-sec, and the hole concentration was $1 \times 10^{18}/cm^3$.

The free growth surface of the thinner films were of optical quality. Thicker films showed a patchiness suggestive of a corresponding patchiness on the NaCl films. However, the NaCl-PbS film

interface was smooth and shiny. This fact is supported by scanning electron microscope pictures. Some thin samples were observed under transmission. Electron microscope moire fringes were observed due to the difference in PbS and NaCl lattice spacing. Also, edge dislocations were observed whose burgers vector was $\frac{a}{2}$ [110].

This technique of growing epitaxic films without thermal strain still requires considerable additional work. However, it promises to be a useful method of producing single crystal layers suitable for technological developments.

Investigators: A. K. Sood and J. N. Zemel

b) Thermoreflectance. The purpose of these experiments was to get a deeper insight into various higher order transitions taking place in PbS and $Pb_xCd_{1-x}S$ using the techniques of modulation spectroscopy and to see their correlation with the calculated band structure of PbS. The technique used for these measurements was to modulate the temperature of the sample and detect the change in reflectivity vs. reflectivity ($\Delta R/R$) of these samples.

The samples prepared for these measurements were in the form of thin films grown by evaporation techniques on NaCl ranging from thickness of 1μ-3μ. A piece of sample of the order of (4mm × 4m) was taken and two strips of Ag-paste were put on the surface to pass ac current through them. The frequency of modulation was picked to be 26 Hz. Some samples were prepared using Scotch-Cast (nonoptical cement) to see if there was any effect due to strains built up in the sample during evaporation. The measurements were taken at 300°K and 77°K.

The structures were found to be much more sharp at 77°K. Some new structures were observed at 77°K which requires some theoretical calculation to explain them.

Similarly, temperature modulation experiments were performed on thin films of PbSe using the same technique. The structure found in this case is very much similar to that of PbS. The experimental plots of $\Delta R/R$ for the PbS and PbSe are shown in Figs. 3-6.

Electric field modulation technique was also used to get $\Delta R/R$ vs. photon energy using samples with MOS configuration. The results obtained were not very conclusive due to bad quality of MOS samples.

The reflectivity measurements of Cardona and Greenaway[5] on PbS and PbSe yield the energies for the first three peaks in units of eV as listed in Table II.

TABLE II

	PbS		PbSe	
	300°K	77°K	300°K	77°K
E_1	1.88	1.85	1.55	1.59
E_2	3.67	3.49	3.12	2.95
E_3	5.3	5.23	4.50	4.65

It is difficult to decide from their experimental data whether the shift of these peaks with temperature is real or due to experimental errors. Identification of the above peaks with our thermoreflectance

spectrum of PbS and PbSe leads to the energies in Table III.

TABLE III

	PbS		PbSe		
	300°K	77°K	300°K	77°K	
E_1	1.92	1.90	1.58	1.58	
E_2	3.72	3.72	3.22	3.20	
E_3	-	-	4.70	4.80	Sample 20(a)
			4.70	4.85	Sample 20(b)

Thus, the E_1 and E_2 transitions are in quite good agreement with the reflectivity spectrum. But the E_3 transitions shows a significant shift from sample to sample.

Certain trends are recognizable in the spectrum of PbS and PbSe. The peaks E_1, E_2, E_3 shift towards higher energy as we go from PbSe to PbS. Both in PbS and PbSe the E_2-peak at room temperature splits up into three peaks at 77°K which implies that E_2-peak is made up of more than one transition at that energy. The splitting is due to different values of their deformation potentials. In the region where the E_3 transition occurs, again we see the splitting into a doublet at liquid nitrogen temperature. But this region has also been found sensitive to the ambients. The spectrum shows a significant pump-down effect, which would require more work to pinpoint the detail of the mechanism.

Gas effect measurement and the effect of carrier concentration on the structure in the 3.5-6 eV range may give us more insight into the origin of these structure. Similar experiments of $Pb_{1-x}Cd_xS$ will be carried out in the future.

Investigators: A. K. Sood and J. E. Fischer

2. $Sn_{1-x}Ge_xTe$ and SnTe

a) Growth and Physical Properties. Epitaxial films have been grown for the $Sn_{1-x}Ge_xTe$ alloy system under near equilibrium conditions employing a modified hot-wall technique. Figure 7 is a schematic diagram of the system designed to achieve the required quasi-equilibrium conditions for the epitaxial growth. The essential part of the system is two separate coaxial tubes made of fused quartz fitted loosely one into the other. One of the tubes contains the source material and the other, the chimney, is used to guide the evaporated molecular beam toward the substrate. The baffle and the neck in the chimney part serve to prevent the evaporant from striking the substrate directly. The oven around the chimney is made of a fused quartz cylinder wound with the nichrome wire as the heater. By carefully controlling the current flowing through the heaters, the right temperature profile can be found such that single crystal films can be grown onto the substrate successfully.

Following is the procedure used to grow the single crystal $Sn_{1-x}Ge_xTe$ films:

1) The source tube is loaded with approximately 5 grams of $Sn_{1-x}Ge_xTe$.

2) The substrate is placed onto the sample holder and the shutter closed.

3) The heaters are turned on to keep the temperatures of the substrate, the baffle and the source at 340°C, 450°C and 400°C respectively.

4) The shutter is opened and the substrate lowered down to the top of the chimney and the outgrowth starts.

5) The substrate is raised up and the shutter closed at the end of the evaporation.

6) Heaters are then turned off and the system is let to cool down to room temperature before the film is taken out of the system.

The end-point material SnTe and the $Sn_{1-x}Ge_xTe$ alloy films grown on both NaCl and KCl substrate are single crystal in nature. X-ray diffraction techniques and scanning electron microscopy have been employed to study the epitaxial films grown.

Figure 8 is a diffractometer recording trace of a 0.44 μm thick SnTe film. Three lines, from (200), (400) and (600) planes respectively, are observed. Lack of peaks from other atomic planes is an evidence of the monocrystalline nature of the films. The lattice constant calculated is 6.315Å. Figure 9 is the x-ray data for a single crystal $Sn_{0.77}Ge_{0.23}Te$ film (d = 1.8 μm) grown on KCl. Because of the comparatively high vapor pressure of GeTe, the growth condition for GeTe is different from that for SnTe and SnTe-rich alloy films. Polycrystalline films, however, have been grown by lowering both the

substrate and source temperature.

Investigators: K. Duh and J. N. Zemel

b) Electrical Properties. Table IV is the result of some of the galvanomagnetic measurements of the $Sn_{1-x}Ge_xTe$ films. All of the measured films are p-type. Figure 10 is the temperature dependence of the Hall coefficient, mobility and conductivity for a .3 μm thick SnTe film. The Hall coefficient increases as the temperature is raised. For the low carrier concentration films the change of Hall constants is even more significant which is expected as a result of the existence of a second band. For the high carrier concentration material, so many carriers are in the lower band even at the nitrogen temperature that no significant change is observed with increasing temperature. This is not so for the low carrier concentration material since most of the holes are in the upper band at low temperature. When temperature is increased, holes are transferred to the lower band. The low carrier concentration films are grown with Sn-rich source material and films have been successfully grown with $p = 1.4 \times 10^{19}$, the lowest ever reported.

The dependence of the galvanomagnetic properties on the growth conditions has also been studied. Figures 11 and 12 are the results after measuring a series of films grown at different source temperatures while the baffle and substrate temperatures were kept constant at 450°C and 250°C, respectively.

As the source temperature is raised both the hole mobility and the conductivity increase, reach to a maximum at around 360°C

TABLE IV

	CARRIER CONCENTRATION (holes/cm^3)	MOBILITY (cm^2/v-s)	CONDUCTIVITY (mho/cm)	HALL CONSTANT (cm^3/coul)	TEMPERATURE (R.T. or N.T.)
SnTe M4	3.2×10^{19}	960	0.49×10^{4}	1.95×10^{-1}	R.T.
	4.2×10^{19}	2,374	1.59×10^{4}	1.50×10^{-1}	N.T.
SnTe J6	3.5×10^{20}	136	0.77×10^{4}	1.77×10^{-2}	R.T.
	3.8×10^{20}	361	2.20×10^{4}	1.64×10^{-2}	N.T.
SnTe J4	5.5×10^{20}	120	1.05×10^{4}	1.14×10^{-2}	R.T.
	6.0×10^{20}	346	3.34×10^{4}	1.04×10^{-2}	N.T.
$Sn_{0.77}Ge_{0.23}Te$ 1A3	7.8×10^{20}	43	5.31×10^{3}	8.01×10^{-3}	R.T.
$Sn_{0.54}Ge_{0.46}Te$ 1A5	1.5×10^{21}	19	4.58×10^{3}	4.12×10^{-3}	R.T.

above which both the hole mobility and conductivity do not change very much. Maximum mobility is obtained when the film is grown at an optimum temperature profile.

Investigators: K. Duh and J. N. Zemel

c) Optical Properties. Both the intraband and interband optical properties of the material have been studied.

1. Intraband Optical Effects - In the infrared region the reflectance and transmittance are measured by a Perkin-Elmer Model 457 grating infrared spectrophotometer. Figure 13 is the typical spectrum obtained.

2. Interband Optical Effects - The interband optical effects are studied by employing the modulation spectroscopy. The experimental setup is the standard one for this kind of work.[6] Monochromatic radiation is reflected at near normal incidence from the surface of the sample into a detector photomultiplier tube is used in the range from 1 eV up to 5.6 eV. For the lower energy range, from .4 to 1.5 eV, a PbS detector is used. The modulation is achieved by passing a modulating current through the sample. In order to obtain a higher modulation efficiency a 26 Hz square wave is used.

Figure 14 is the thermoreflectance spectrum of SnTe at room temperature. This spectrum is richer in identifiable structure than previously obtained electroreflectance results obtained by Aspnes.

Figs. 15 and 16 are the thermoreflectance of the GeTe and $Ge_{0.23}Sn_{0.77}Te$ samples. This work is still under progress. Kramers-Kronig analysis is being undertaken to better identify the structure and to better understand the optical properties of these materials.

Investigators: K. Duh and J. E. Fischer

3. PbO_xS_{1-x}

Films of PbO_xS_{1-x} of various compositions were grown during this period. The physical properties of the films were characterized by x-ray analysis, electron microscopy, and Auger spectroscopy. If is difficult at the present time to obtain exact values for oxygen concentration although it is hoped that Auger spectroscopy will yield this information.

Photoconductivity measurement on the PbO_xS_{1-x} films showed the appearance of a strong peak on the long wavelength side of the PbS peak. The strength of this peak is proportional to the oxygen concentration (Figs. 17-19). Tables V and VI give some of the electrical and photoconductive data obtained on these films. The sensitivity was measured both at the PbS and the oxygen generated peaks. The film MS 25 was pure PbS and the rest are PbO_xS_{1-x} with D2 and D-3 having the lowest and highest oxygen concentration respectively. All except D3 were n-type.

The photoconductivity data appear to indicate the oxygen introduces localized trapping levels in the band gap of PbS. The considerable increase in the responsivity cannot be explained by

TABLE V. Values of lifetime and sensitivity at a wavelength below the oxygen created peak of the photoresponse of PbO_xS_{1-x} along with mobility and Hall coefficients at 77 and 300°K.

Film	λ_p in microns		λ_{ox} in microns		τ in ns.		Sensit. $\mu v/\mu w\ cm^{-2}$		Mobility $cm^2/V\text{-}Sec$		P_H	
	300°K	77°K	300°K	77°K	300°K	77°K	300°K	77°K	300°K	77°K	300°K	77°K
MS25	3.05	3.2	–	–	20	80	.0024	.01	640	3500	2.7	2.7
D2	3.03	3.86	4.4	4.4	20	740	.00026	.03	410	2500	2.7	2.7
D3	3.5	3.5	4.0	4.4	13.7	16000	.0044	1.54	150	280	7.6	9.2
D31	3.5	3.8	4.4	4.7	3.72	3500	.0015	.08	140	260	6.2	7.5
D41	2.64	2.64	4.4	4.66	–	264	.0001	.03	260	480	5	5.2

TABLE VI. Room temperature values of lifetime and sensitivity at the oxygen created peak of the photoresponse of PbO_xS_{1-x}.

Film	Sensitivity at 300°K $\mu v/\mu w\ cm^{-2}$	τ in μs at 300°K
D-3	2.37	19.55
D-31	1.87	2.7
D-41	.034	.178

variation of PbS lifetime. A resulting impurity type band, caused by the overlap of these localized levels can explain the behaviour of the photoconductivity. The same model was used to explain the temperature dependence of the carrier concentration for both n- and p-type materials (Fig. 20).

The variation of the absorption coefficient with wavelength (Figs. 21, 22), exhibits regions corresponding to direct and indirect transitions, consistent with the proposed model.

Extensive work is being carried out now to obtain more information regarding the nature of these localized states.

THEORETICAL RESEARCH

1. Band Structure of IV-VI Alloys

A full-relativistic augmented-plane-wave program (D) has been developed which solves the Dirac's equation. This program has been successfully tested on SnTe and the results compared with those of the previous APW calculations where the relativistic corrections were introduced by perturbation technique (P).[7,8] In order to compare the nonrelativistic results obtained by the two different methods (E^D_{NR} and E^P_{NR}) the velocity of light was set equal to infinity in the full-relativistic calculations to obtain E^D_{NR}. Then the relativistic results (E^D_R and E^P_R) were compared to check the relativistic corrections. The results for points Γ and L in the Brillouin zone are given in Table VII. Although the same potential was used in both calculations, the new formalism requires the potential on a logarithmic mesh while

the previous program uses it on a semilinear mesh. Thus the original potential had to be interpolated to convert it to a logarithmic mesh. The other difference was a slight change in the radii of APW sphere, again necessitated by the difference in the radial mesh required by the two programs. The error introduced by the above two factors is in all likelihood responsible for the difference between the two set of nonrelativistic results. The upper limit for this discrepancy is .1 eV. The relativistic corrections show a larger discrepancy, however the limiting difference is 10% of the size of the relativistic correction and is generally much less. Again the two sources of error in comparison may be responsible for part of this discrepancy. Thus we see that the original band calculations for the IV-VI compounds were indeed quite accurate. The only need for going to the new formalism is its appropriateness for the alloy band calculation.

Tests are also in progress to determine the effect of using Waber's[9] relativistic atomic wavefunctions in the construction of the periodic crystal potential in contrast to the presently used, non-relativistic atomic wavefunctions of Herman and Skillman.[10]

We are now in a position to start the "virtual crystal" band calculations for the IV-VI alloys.

Investigators: R. Lasseter, S. Rabii

TABLE VII. Comparison of the energy bands for SnTe and Γ and L obtained by the Dirac's equation and the perturbation technique. Energies are in units of Rydbergs.

SINGLE GROUP	NONRELATIVISTIC		RELATIVISTIC		RELATIVISTIC CORRECTION		DOUBLE GROUP
	E^P_{NR}	E^D_{NR}	E^P_R	E^D_R	$E^P_R-E^P_{NR}$	$E^D_R-E^D_{NR}$	
L'_3	-.486	-.488	-.504	-.507	-.018	-.019	L_4^-, L_5^-
			-.525	-.530	-.039	-.042	L_6^-
L_1	-.485	-.489	-.568	-.580	-.083	-.091	L_6^+
L'_2	-.562	-.565	-.617	-.624	-.055	-.059	L_6^-
L'_3	-.651	-.652	-.679	-.682	-.028	-.030	L_4^+, L_5^+
			-.720	-.727	-.069	-.075	L_6^+
Γ_1	-.034	-.035	-.111	-.121	-.077	-.086	Γ_6^+
Γ'_2	-.230	-.231	-.230	-.231	0	0	Γ'_7
Γ'_{25}	-.257	-.259	-.264	-.267	-.007	-.008	Γ_8^+
			-.264	-.263	-.007	-.004	Γ_7^+
Γ_{15}	-.264	-.272	-.291	-.298	-.027	-.026	Γ_8^-
			-.343	-.357	-.079	-.085	Γ_6^-
Γ^{15}	-.655	-.659	-.684	-.689	-.029	-.030	Γ_8^-
			-.743	-.755	-.088	-.096	Γ_6^-
Γ_1	-.738	-.737	-.894	-.910	-.156	-.173	Γ_6^+

2. SnTe and the Lead Chalcogenides

The calculation of the deformation potentials for Σ extrema of these compounds has been concluded. We can thus predict the behaviour of these extrema under various strains. The matrix elements have been calculated for isotropic, [111], [1$\bar{1}$1], [100], and [001] deformations. These results are being applied to identify the peaks in the modulation spectra of the IV-VI compounds and will be used to explain the temperature dependence of their galvanomagnetic properties.

Investigator: S. Rabii

PHYSIOCHEMICAL STUDIES OF THE PbS-PbO SYSTEM

In the past year significant progress has been made in the understanding of the PbS-PbO system. The experimental system has been completed and a large number of informative kinetic studies have been performed.

The bulk of the experimental work has been in the measuring of the weight gain of pressed pellets of PbS in various oxidizing environments. The PbS used to date, has included reagent grade, high purity "5N", and naturally occurring PbS (galena). The pellets have been prepared by pressing PbS powder of known grain size. The "as pressed pellets" are approximately 86% theoretical density. Scanning electrode microscopy has clearly shown that these pellets have a true surface area much greater than the geometric area. Our best estimates indicate that the surface area of the "as pressed pellet" is approximately 100 times greater than the geometric surface area.

Kinetic studies have been performed to date, below 800°C since the sublimation of PbS becomes significant above 800°C. The kinetic data has been reproducible within ±1% over a 400-800 cc/min. flowrate of gas mixtures. A number of interesting preliminary results have been observed from the kinetic studies involving the PbS pellets. Under gas flowing conditions at which $PbO \cdot PbSO_4$ is stable, a direct dependence on oxygen pressure is observed. This normally expected type of behavior is in direct contradiction to previously reported work in the literature. The oxidation of PbS pellets in a simple oxygen atmosphere indicates that the impurity content of the PbS has a significant effect on the initial weight gain kinetics.

Some X-ray work has been performed in an attempt to identify the various reaction products. To date, the X-ray analysis work has not been conclusive. The major problems have been the facts that very little reaction product is obtained and the product is difficult to remove from the partially reacted PbS pellet. Further X-ray work will be performed on the reaction products formed on both pellets and single crystals of PbS.

Future experiments contemplated at the present time include weight gain measurements of single crystals of PbS and weight change measurements in which the starting material will be one of the reaction products such as $PbSO_4$ or PbO.

Investigators: G. Belton and W. Kreuger

ELASTIC SURFACE WAVE STUDIES

This project has as its overall scientific objective the investigation of various electronic and elastic properties of semiconductors in the form of epitaxial films using surface acoustic waves (such as Rayleigh waves).

Our initial research has been mainly involved with the fabrication of interdigital transducers and the launching of surface waves into semiconductor films. So far we have been able to generate 200 MHz Rayleigh waves with transducers of aluminum interdigital arrays on quartz. A good deal of time has been spent learning the techniques of working with photoresist and mechanical masks, two different methods of evaporating the aluminum arrays onto the quartz. The electrical characteristics of these transducers have been thoroughly studied.

We are presently learning the techniques of growing CdS films and growing IV-VI compounds on CdS for the generation of Rayleigh waves into the IV-VI films. This development stage is nearly completed.

Investigators: T. E. Thompson and F. J. Bogacki

REFERENCES

1. H. Holloway and E. Logothetis, J. Appl. Phys. 71, 3543 (1970).

2. R. F. Bis, A. Rodalakis, and J. N. Zemel, Rev. Sci. Instr. 36, 626 (1965).

3. R. B. Schoolar and J. N. Zemel, J. Appl. Phys. 35, 1848 (1964).

4. R. B. Schoolar and R. Riedl, J. Appl. Phys. 39, 5086 (1968).

5. M. Cardona and D. L. Greenaway, Phys. Rev. 133, A1685 (1964).

6. E. Matatagai, A. Thompson and M. Cardona, Phys. Rev. 176, 960 (1968).

7. S. Rabii, Phys. Rev. 167, 801 (1968).

8. S. Rabii, Phys. Rev. 182, 821 (1969).

9. D. Liberman, J. T. Waber and D. T. Cromer, Phys. Rev. 137, A27 (1965).

10. F. Herman and S. Skillman, Atomic Structure Calculations, Prentice-Hall, Englewood Cliffs, New Jersey (1963).

PUBLICATIONS

1. Y. Ota and S. Rabii, "Carrier Concentration Dependence of the Optical Parameters of SnTe Epitaxic Films at Room Temperature", presented at the Conference on the Physics of Semimetals and Narrow Gap Semiconductors, Phys. Chem. of Solids Supplement No. 1, 32 343 (1971).

2. Y. Ota and S. Rabii, "Band Structure of SnTe", presented at the Conference on the Physics of IV-VI Compounds and Alloys, Phila., March 24-25, 1972, to be published in the Journal of Nonmetals.

3. S. Rabii, "Band Structure of IV-VI Alloys", J. of Vac. Sci. & Tech. 8, 1, Jan.-Feb. 1971.

4. M. Paić and V. Paić, "Formation of Pb During Epitaxial Growth of PbS on KCl in a Vitreous Silica Hot Wall System", presented at the 1972 Int'l. Conf. on Thin Films, 1972, to be published in Thin Solid Films.

5. H. Rahnamai, Y. Ota and J. N. Zemel, "Effect of Atomic H on Epitaxic Films of SnTe", accepted for publication in Thin Solid Films, 1972.

6. A. Sood and J. N. Zemel, "A Multilayer Approach to Epitaxic Growth in Lead Salts", Journal of Vac. Sci. & Tech. 9, 1 (1971), pg. 234.

7. M. Paić, V. Paić, K. Duh and J. N. Zemel, "Quasi-Static Growth of PbS Epitaxic Films", Thin Solid Films 12, 2 (1972), pp. 419-425. (Presented at the 1972 International Conference on Thin Films, Venice, Italy, 1972).

8. F. J. Bogacki, A. K. Sood, C. Y. Yang, S. Rabii and J. E. Fischer,

"Thermoreflectance of IV-VI Compounds", submitted to the First International Conference on Modulation Spectroscopy, to be held in Tucson, Arizona, November 1972.

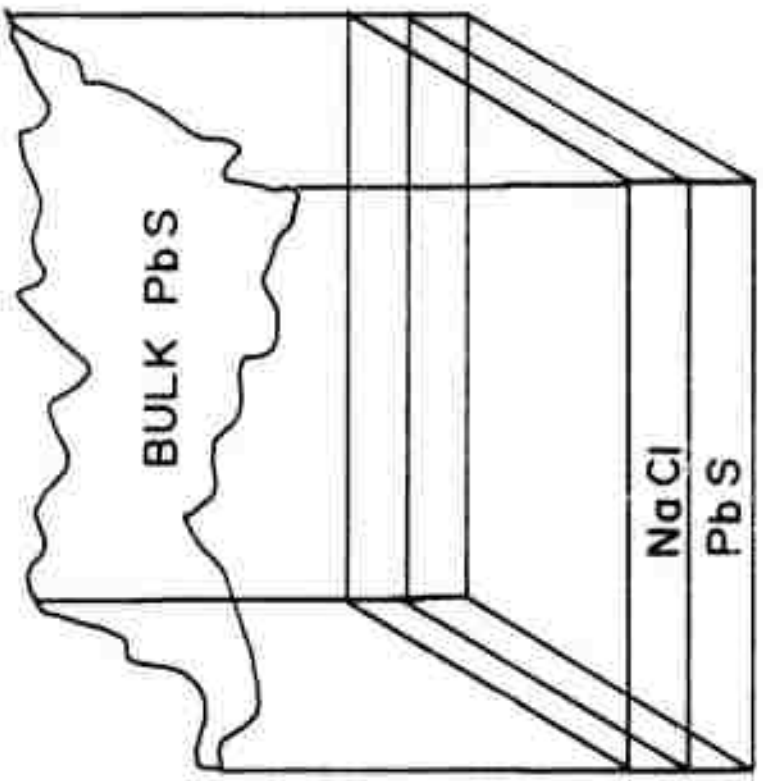

Fig. 1 Parting Layer Technique.

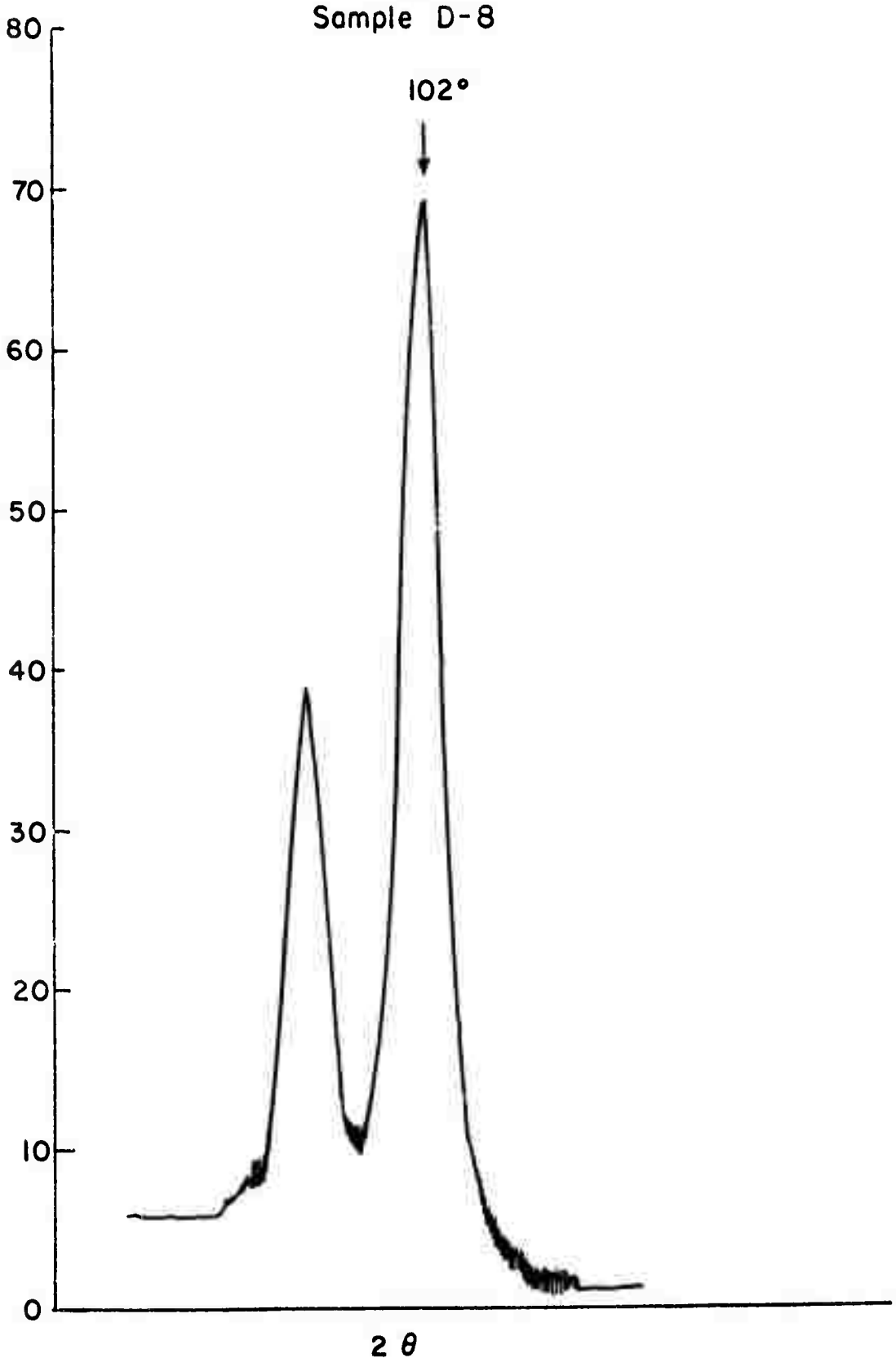

Figure 2. Bragg diffractometer recording for (600) planes of PbS film.

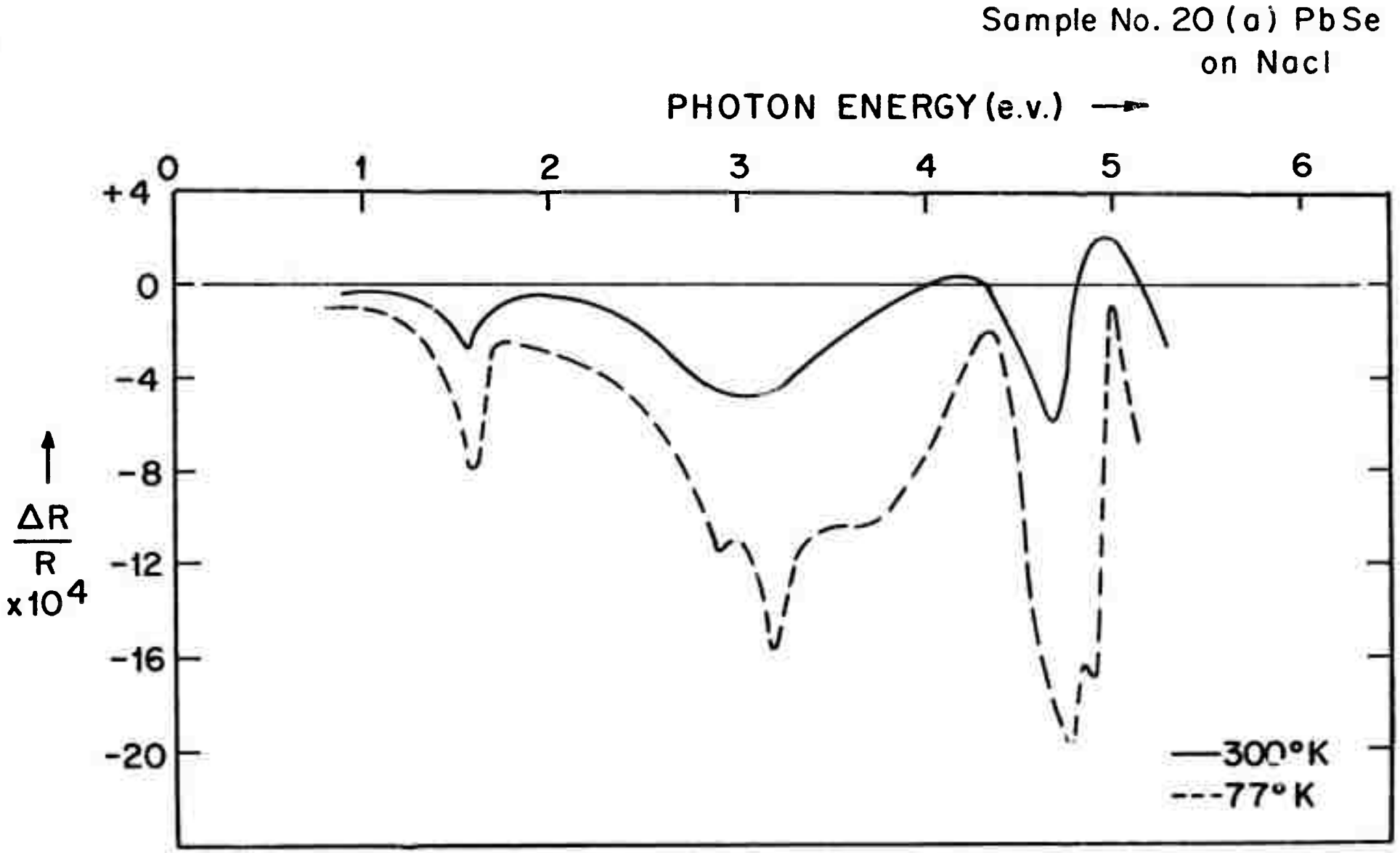

Figure 3. Thermoreflectance Spectrum of PbS Sample No. 20(a).

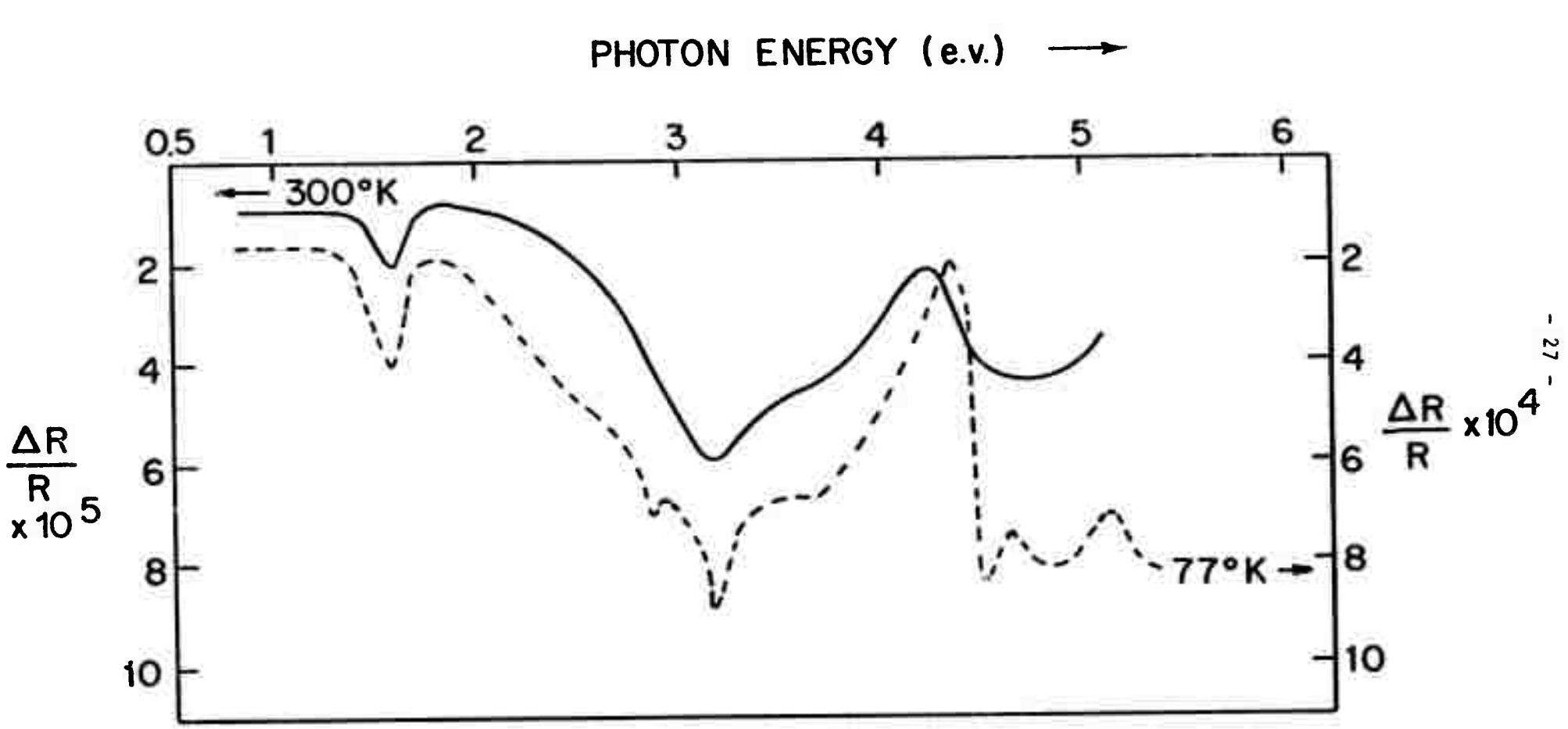

Figure 4. Thermoreflectance Spectrum of PbS Sample No. 20(b).

Sample No. 25 (PbSe)
on NaCl.

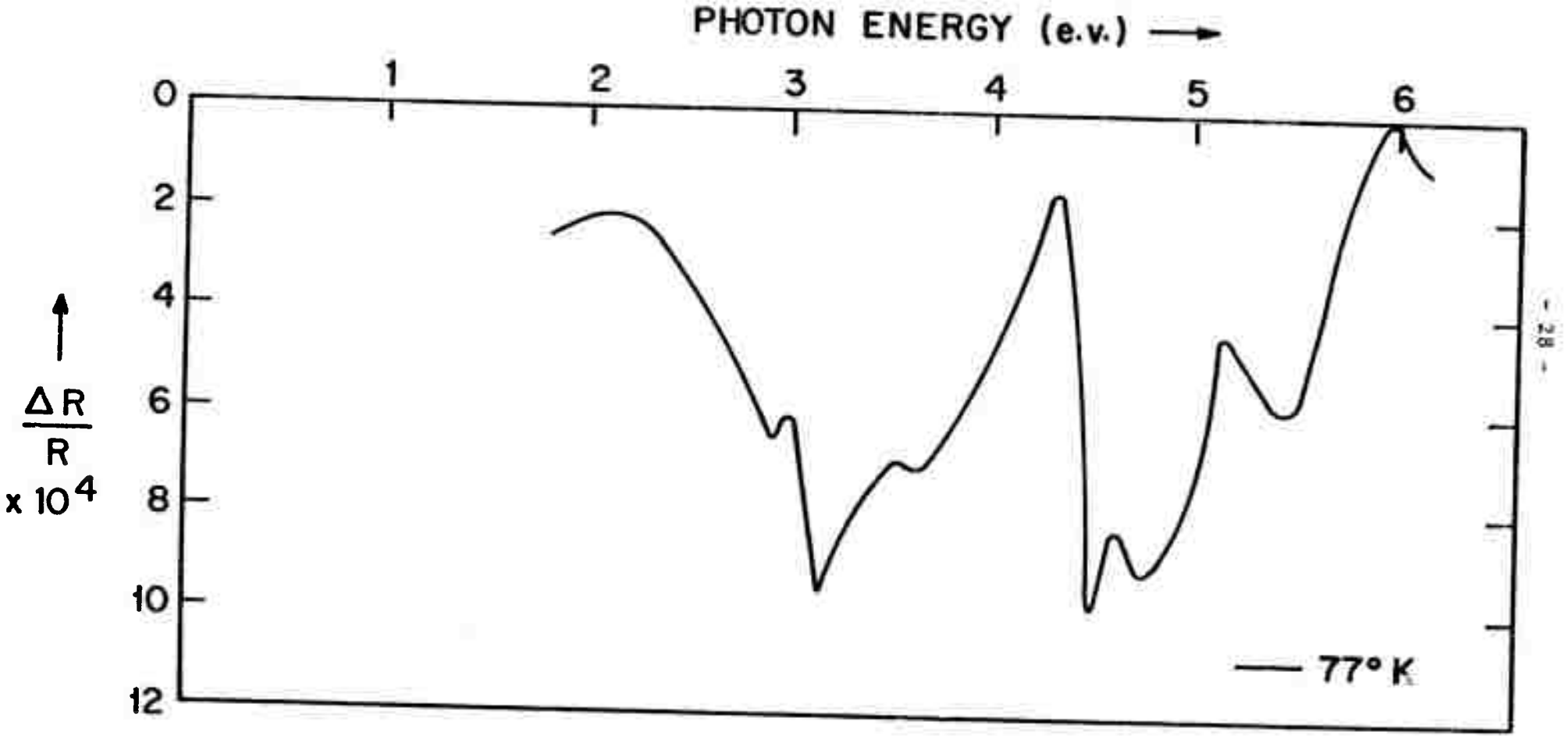

Figure 5. Thermoreflectance Spectrum of PbS Sample No. 25.

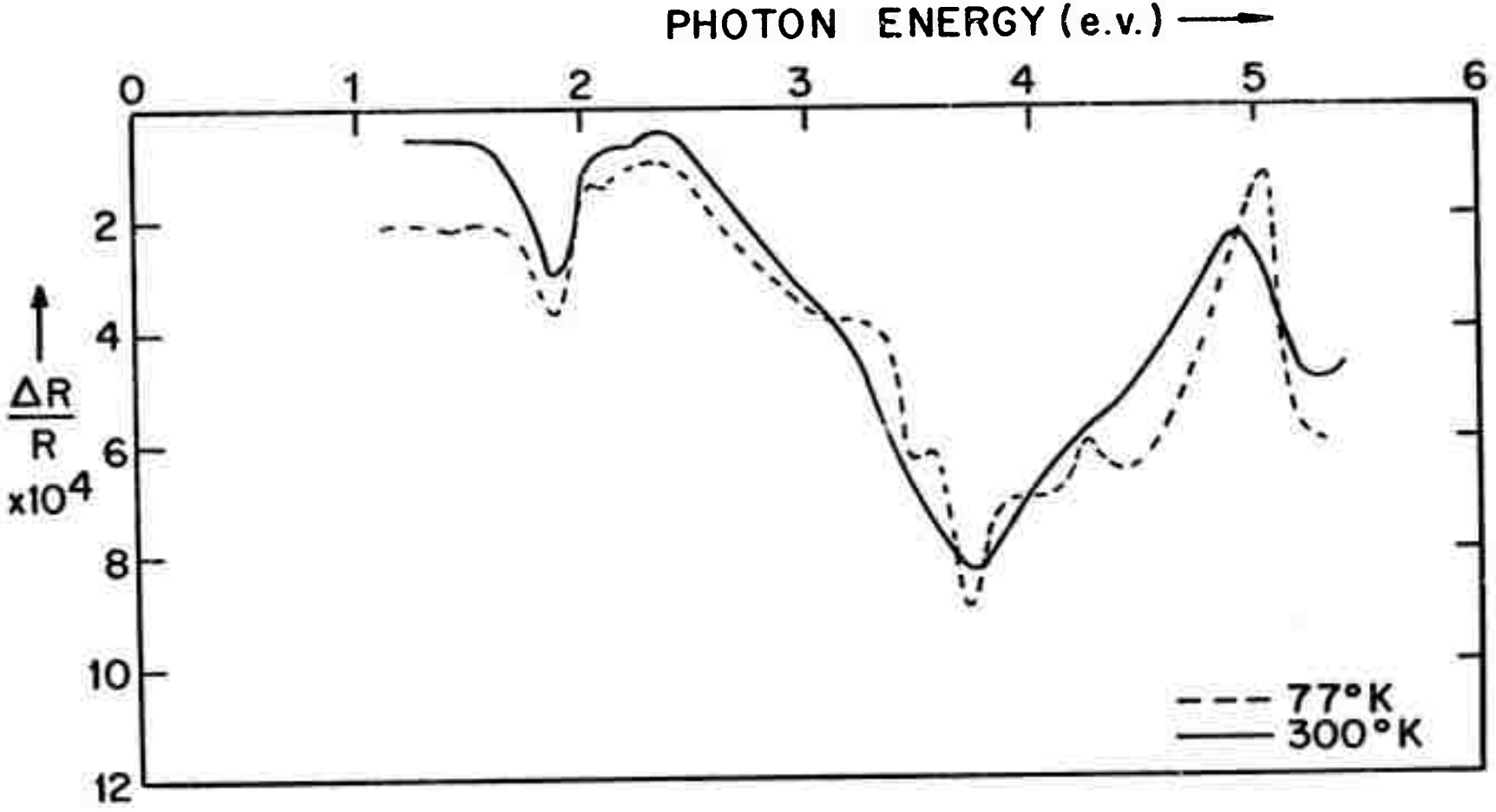

Figure 6. Thermoreflectance Spectrum of PbS Sample No. B-10.

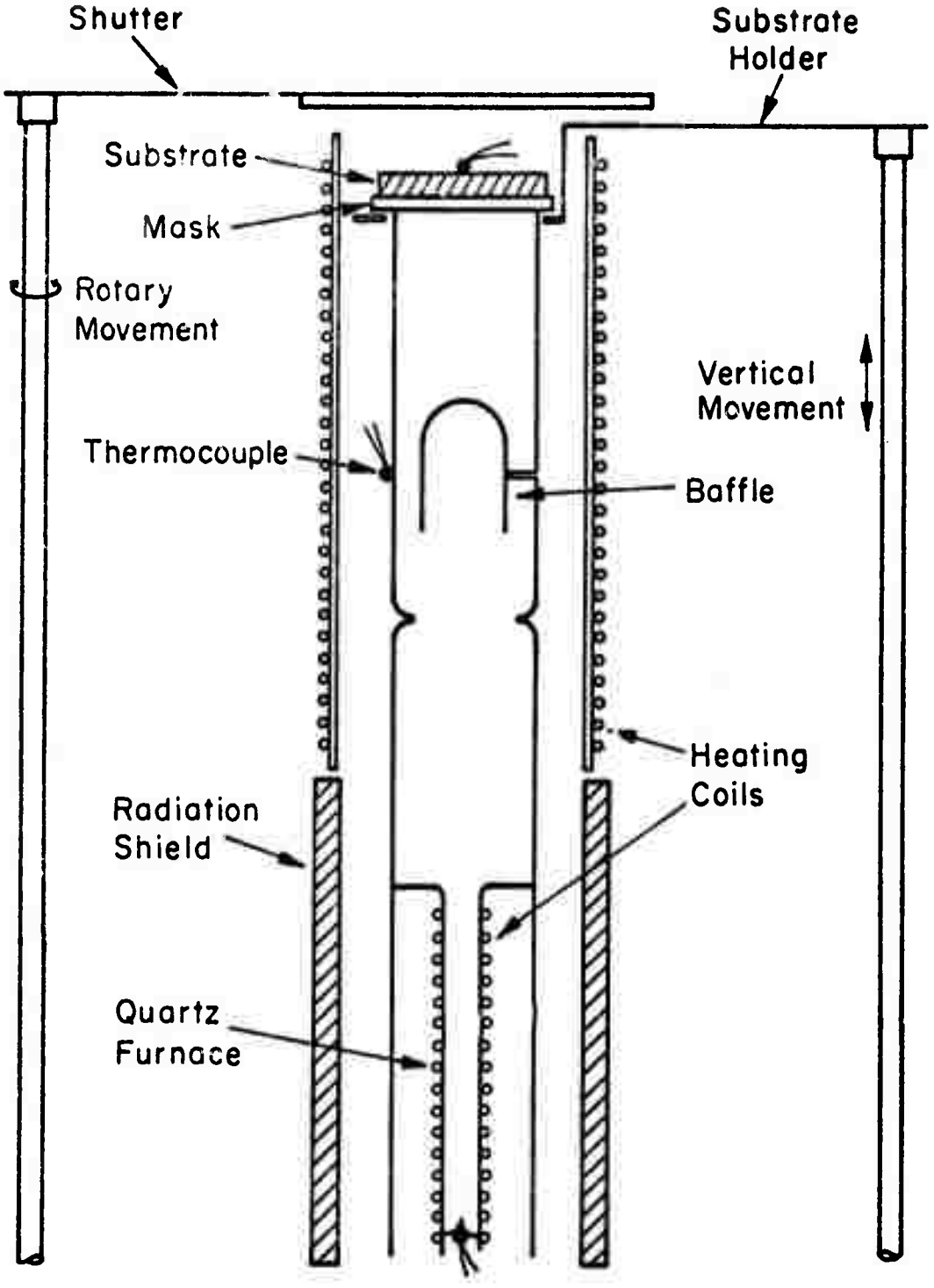

Figure 7 Hot Wall Evaporation System

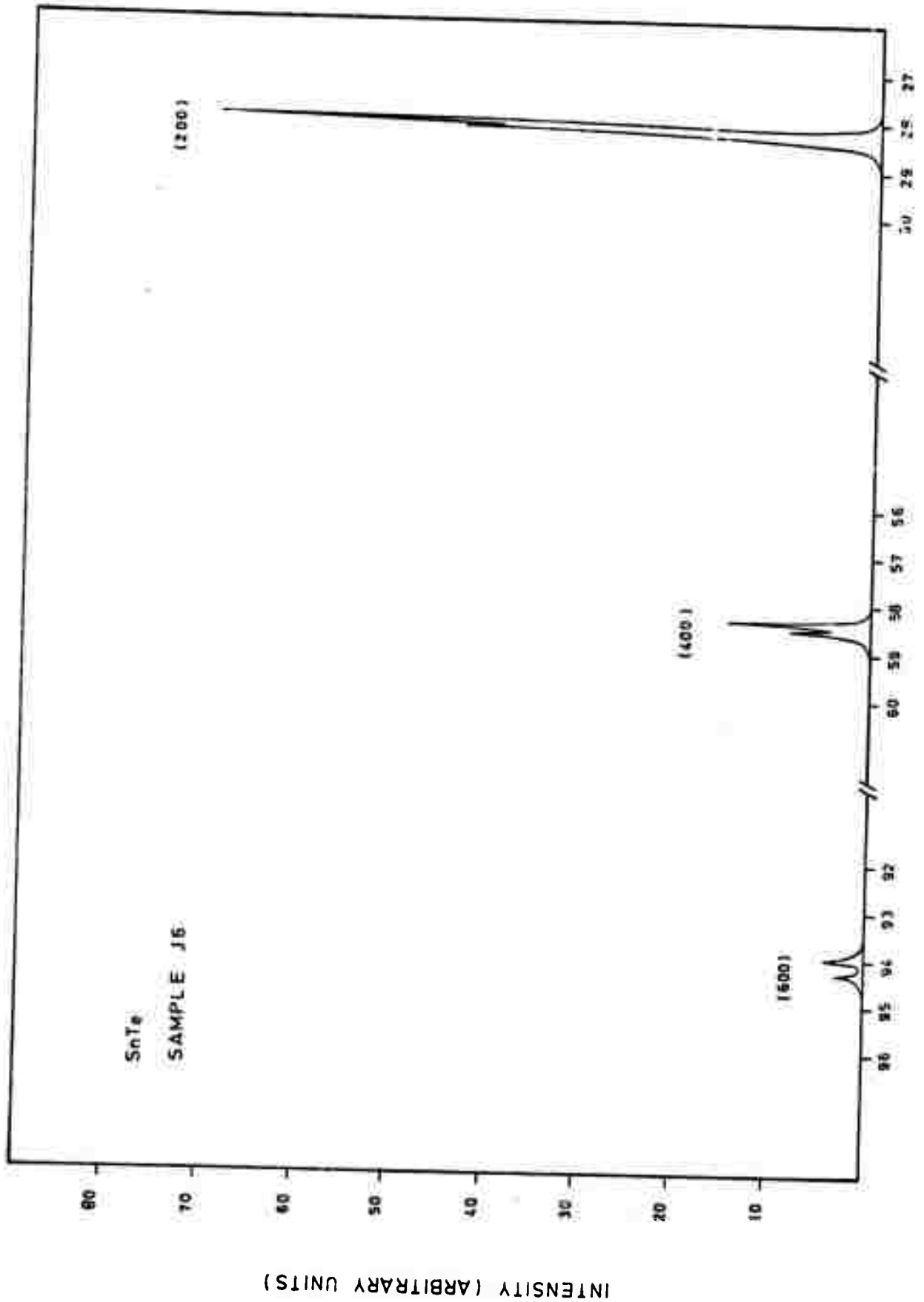

Figure 8. Bragg diffractometer recording of a 0.44 μm SnTe film.

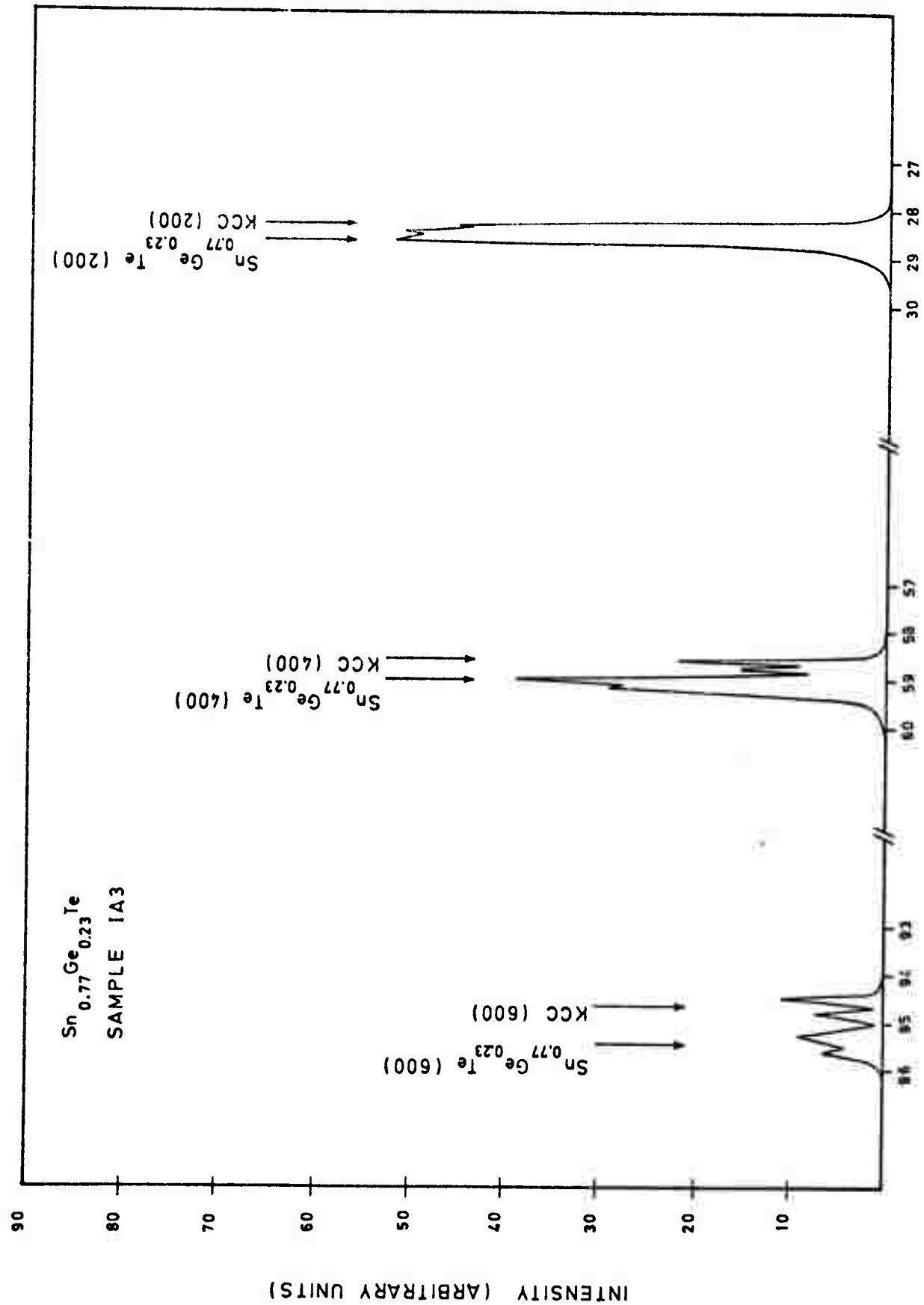

Figure 9. Bragg diffractometer recording of a 1.8 μm $Sn_{0.77}Ge_{0.23}Te$ film.

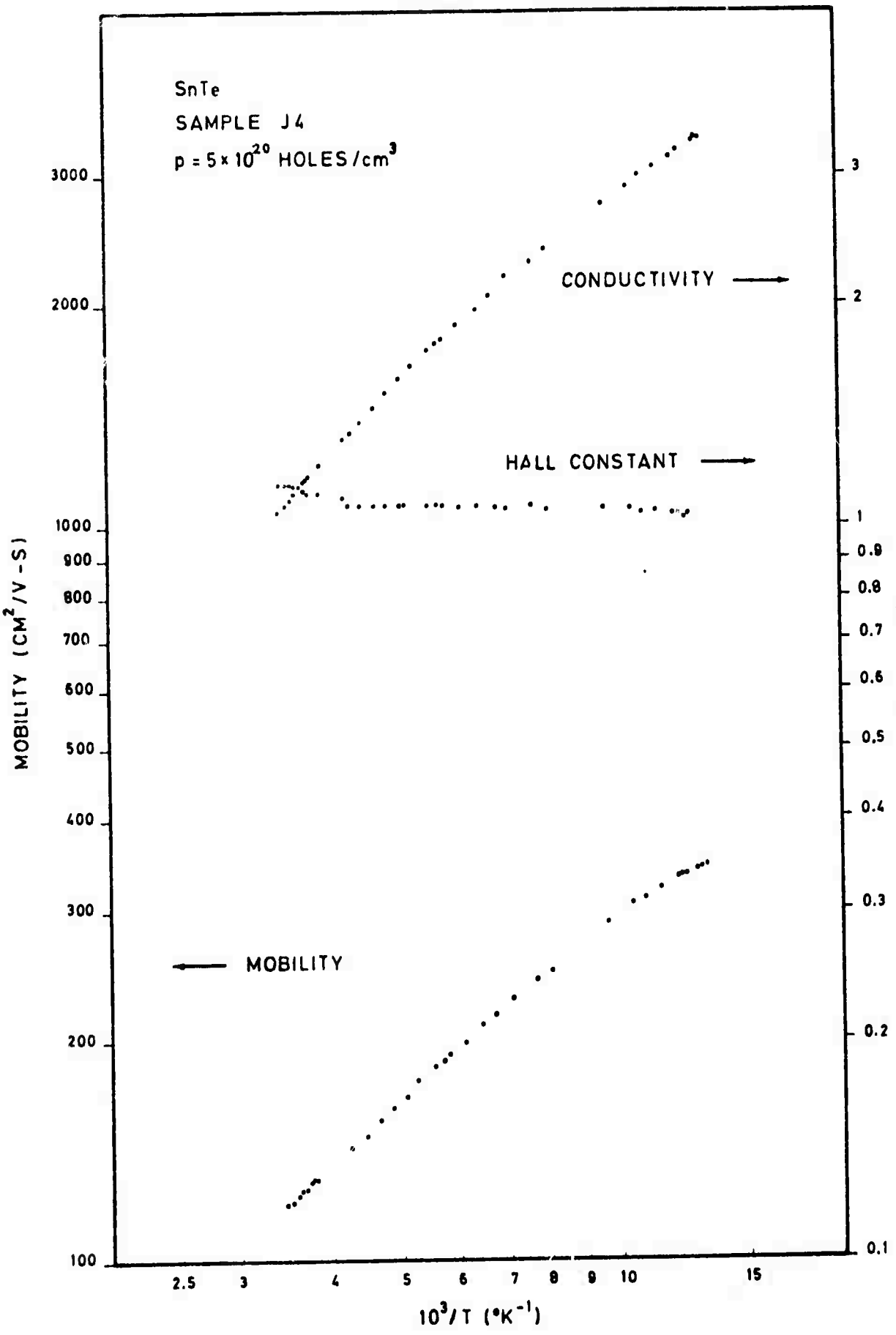

Figure 10 HALL CONSTANT

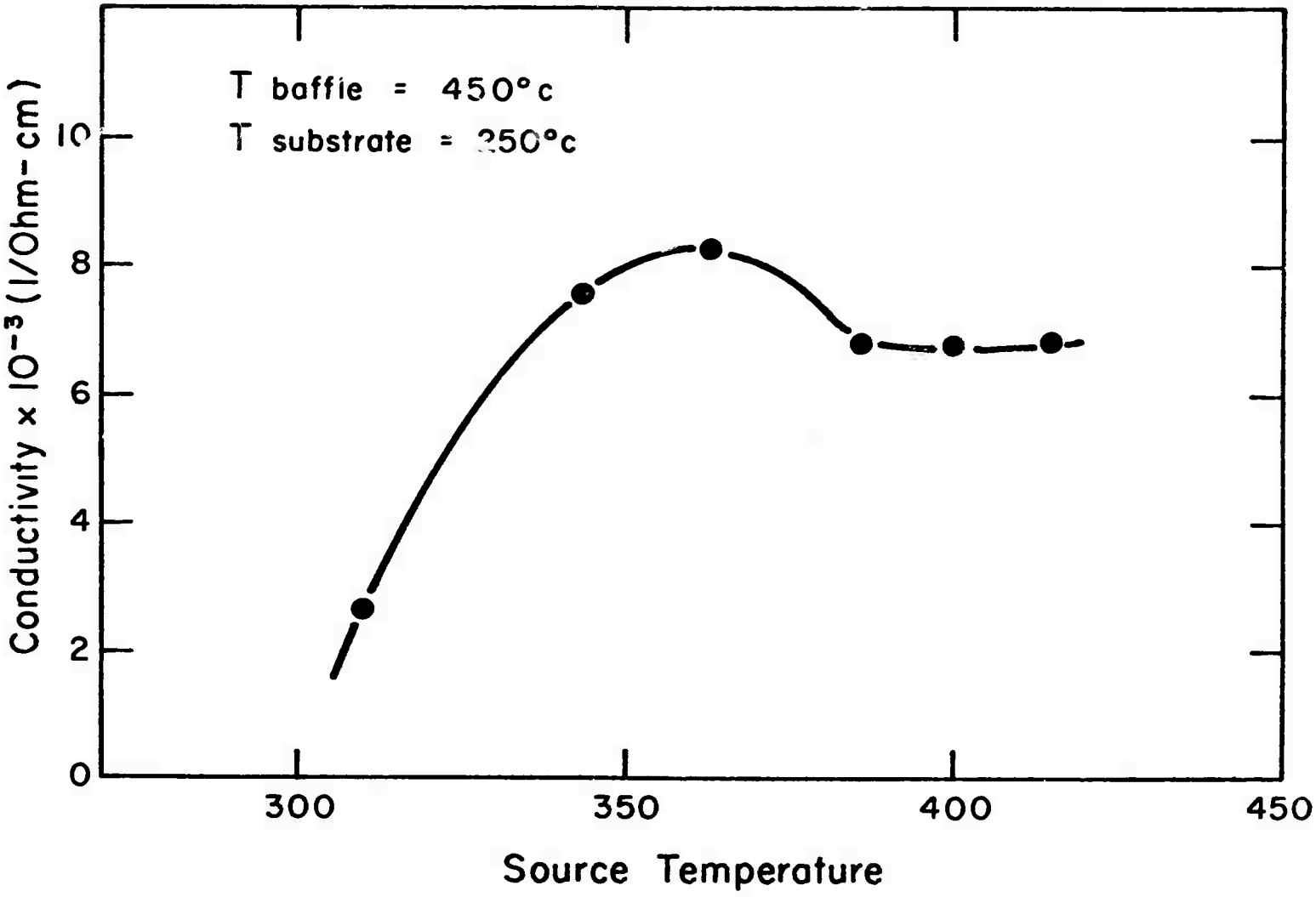

Figure 11 Conductivity of a number of films as a function of source temperature.

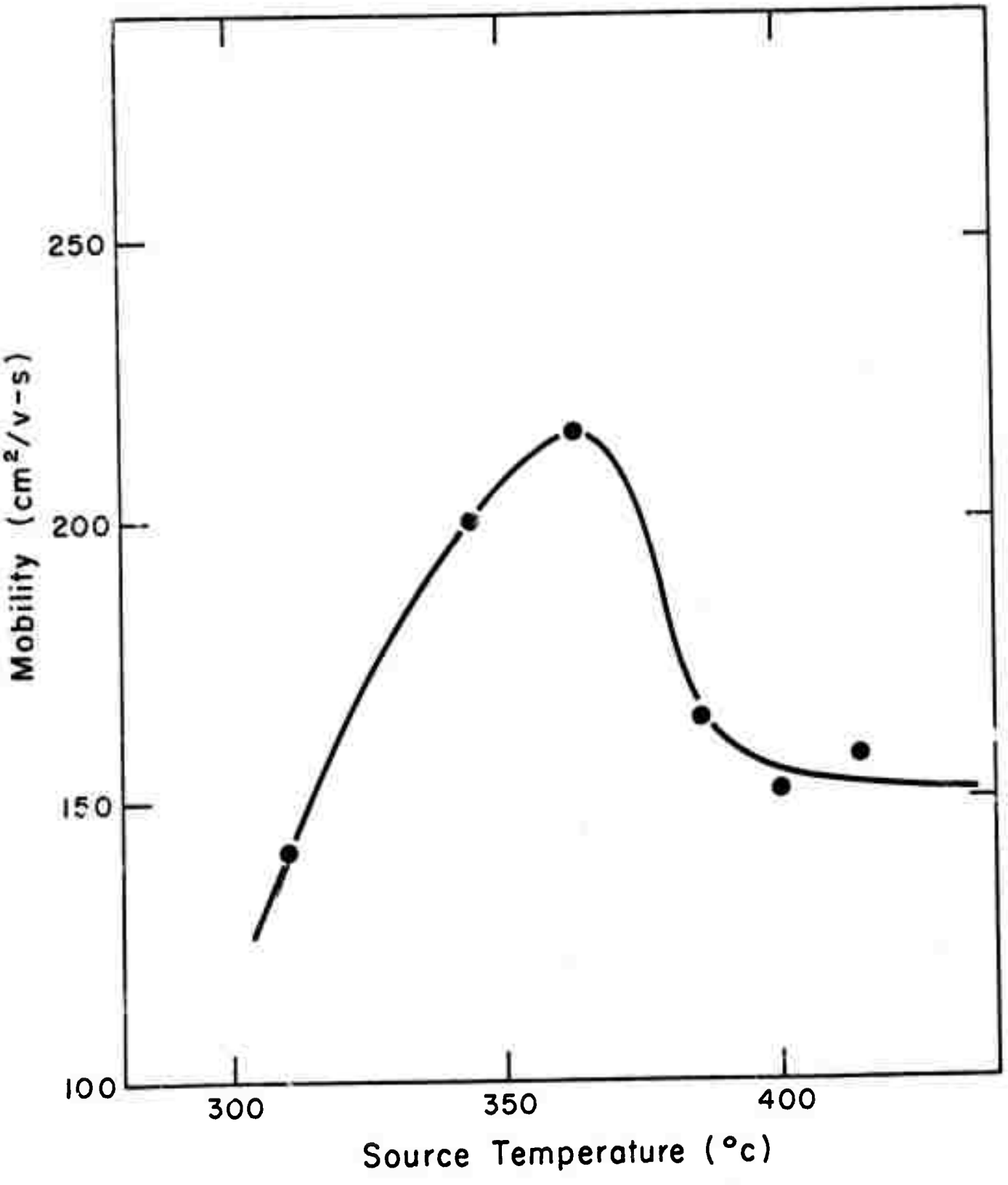

Figure 12. Mobility of a number of films as a function of source temperature.

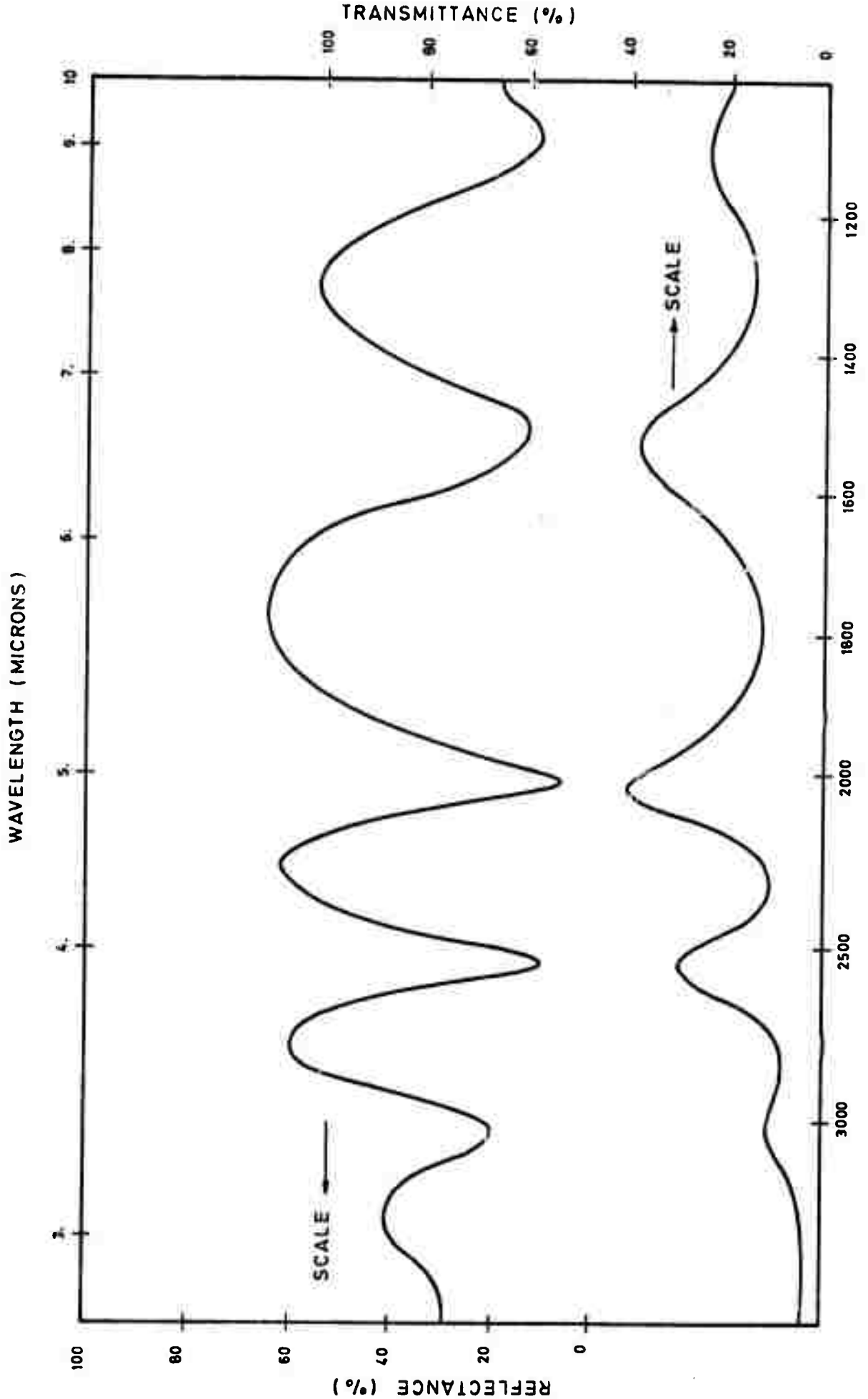

Figure 13. Infrared reflectance and transmittance of SnTe.

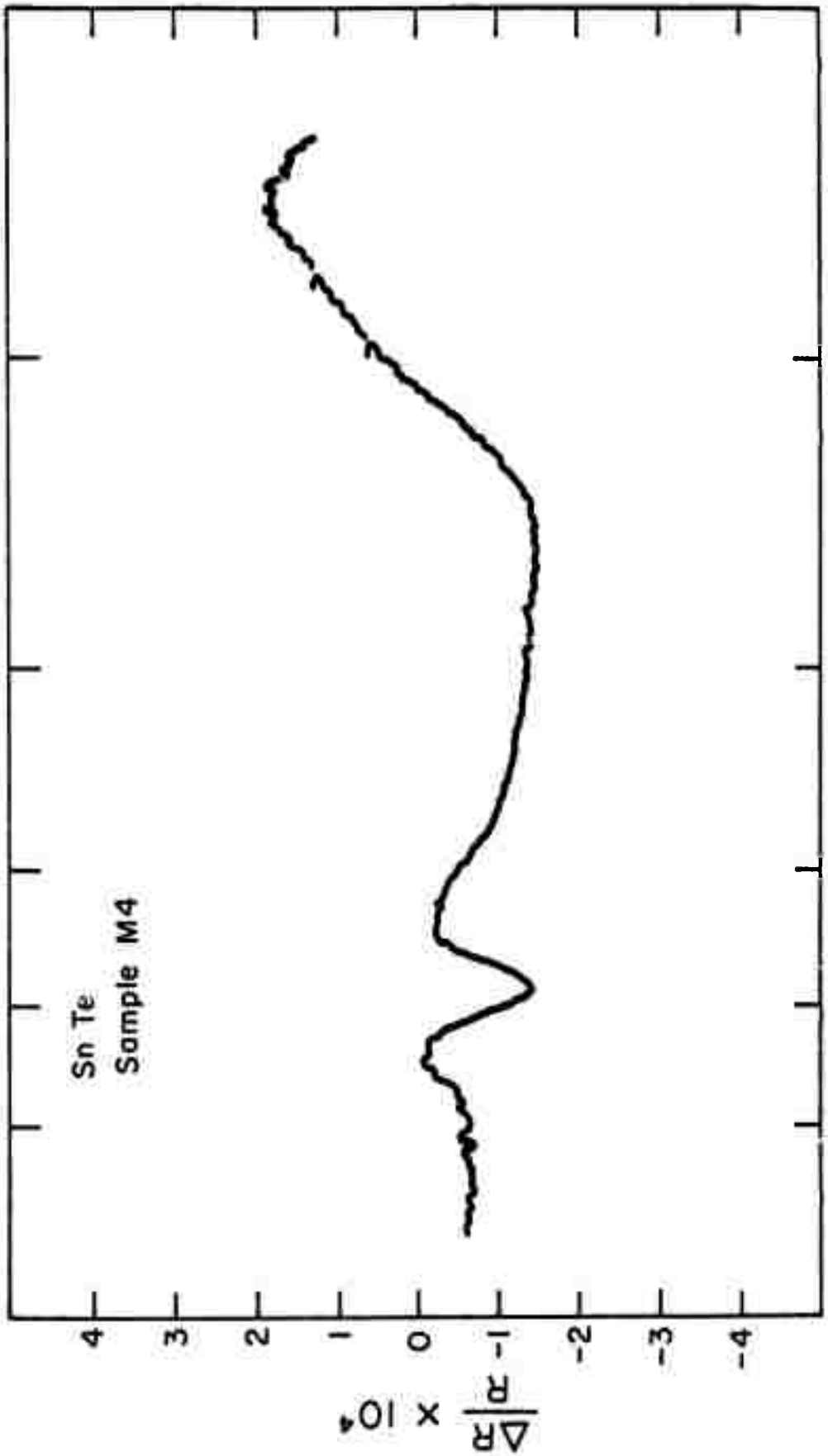

Figure 14 Thermoreflectance spectrum of Sn Te at room temperature

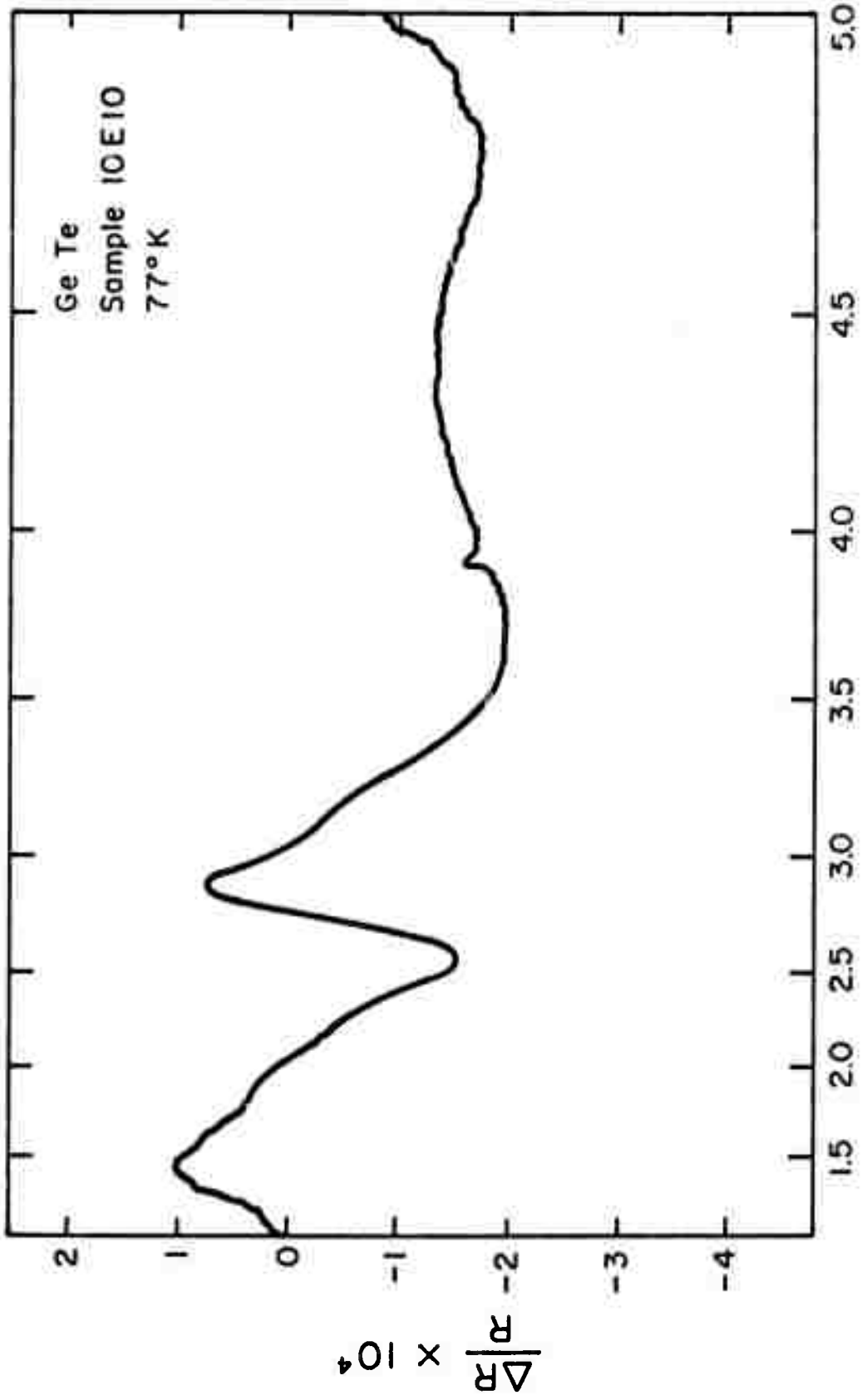

Figure 15. Thermoreflectance of GeTe.

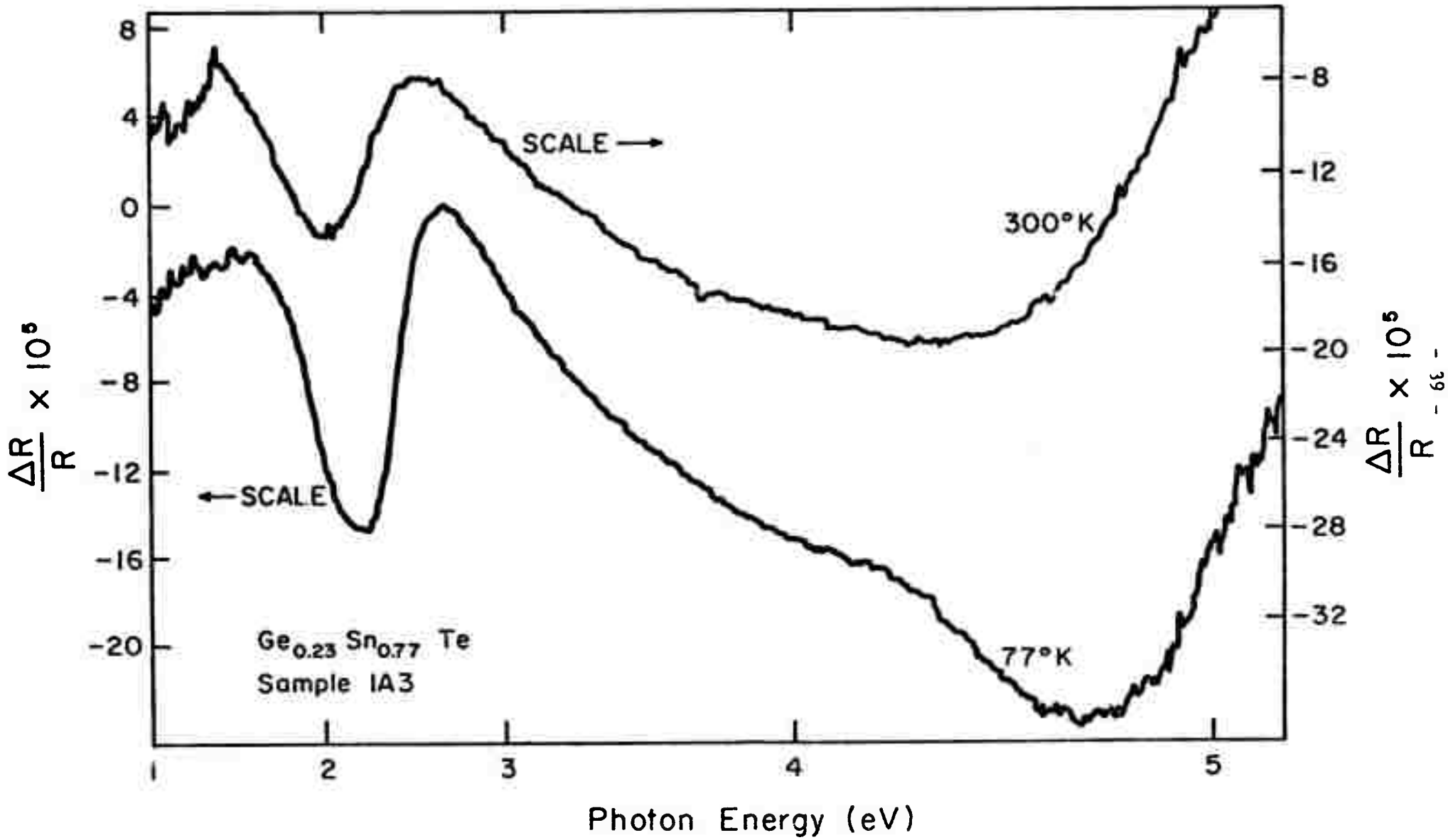

Figure 16. Thermoreflectance of $Ge_{0.23}Sn_{0.77}Te$

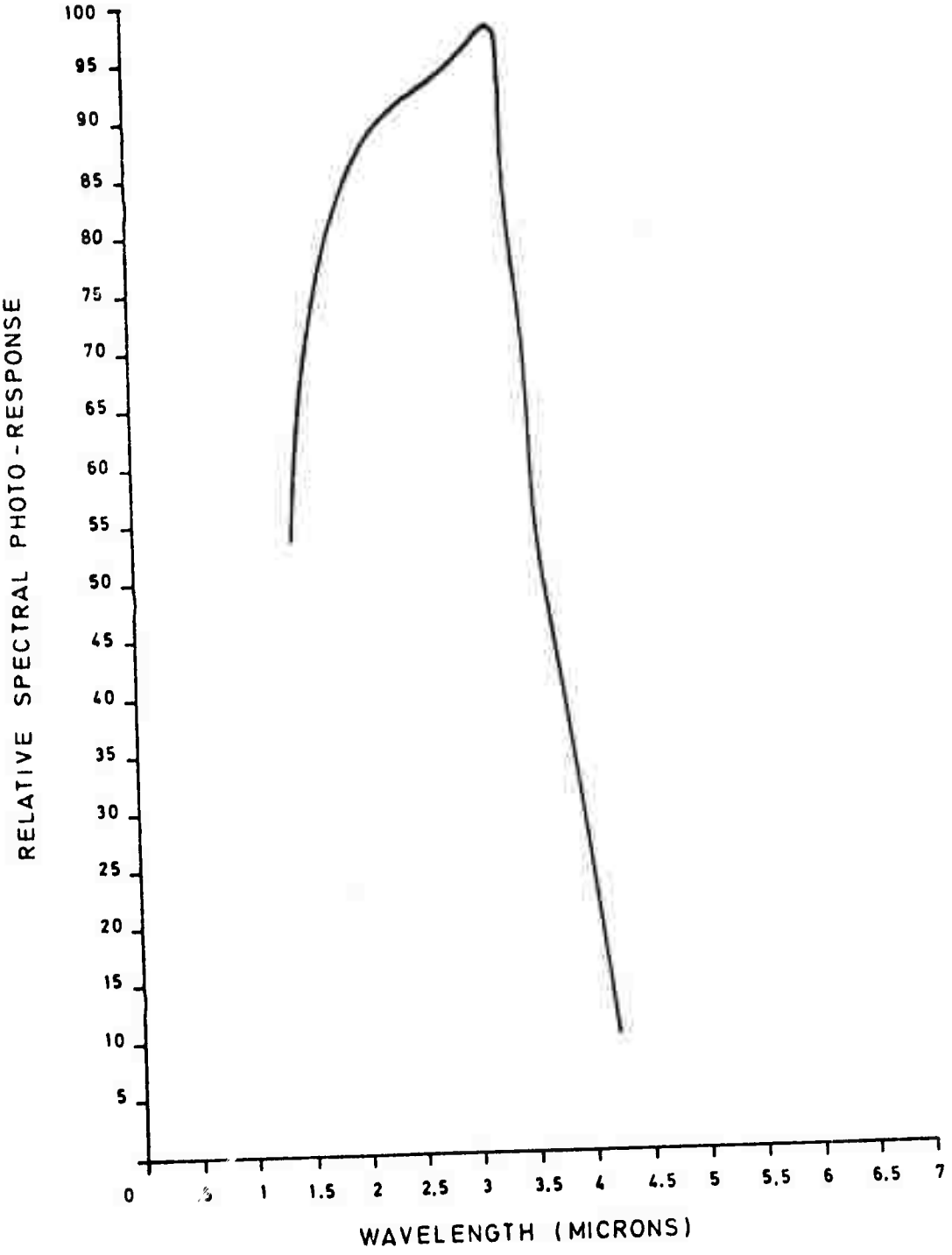

Figure 17. Relative spectral photoresponse of a PbS film

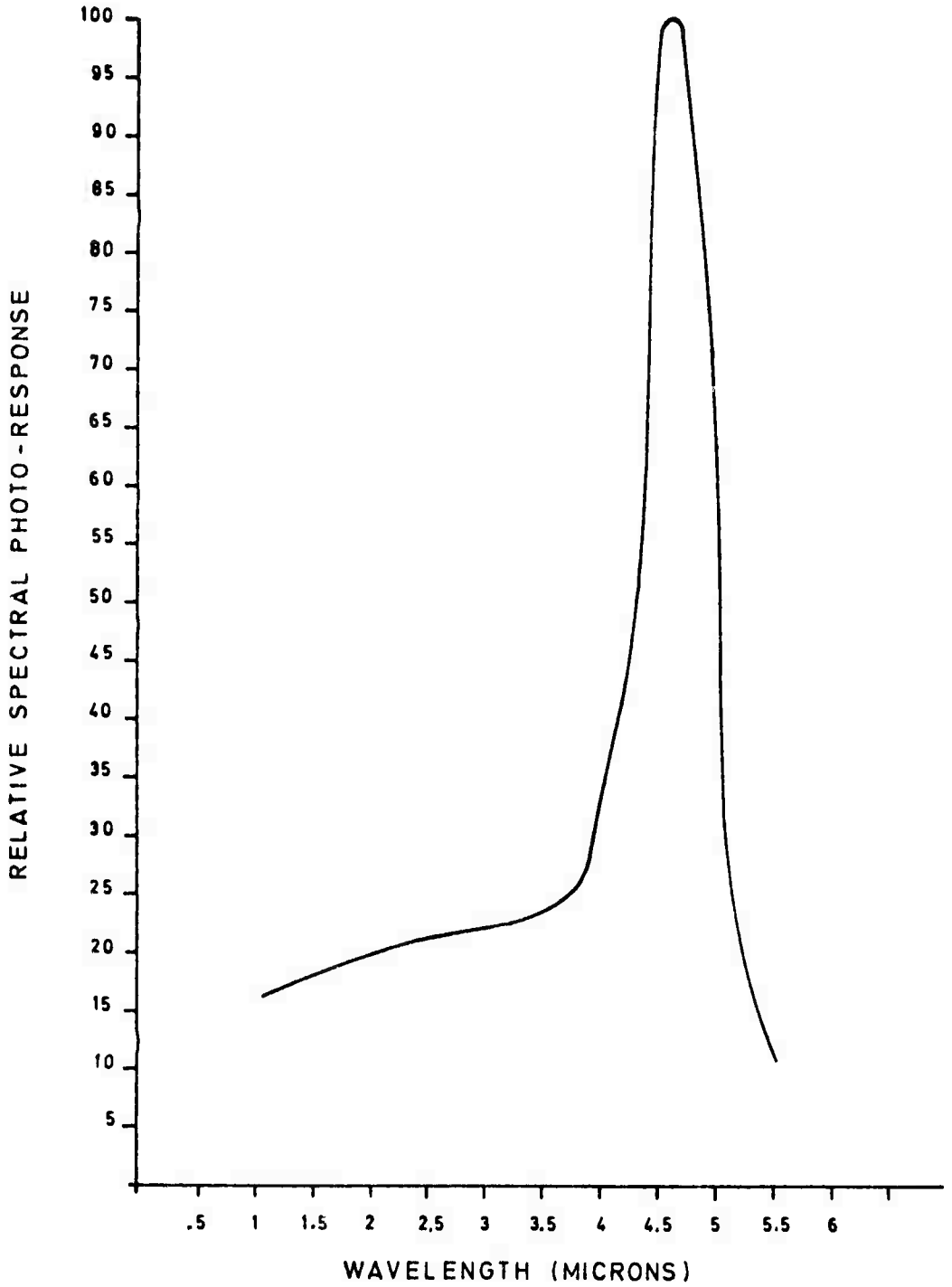

Figure 18. Relative spectral photoresponse of an n-type PbO_xS_{1-x} film.

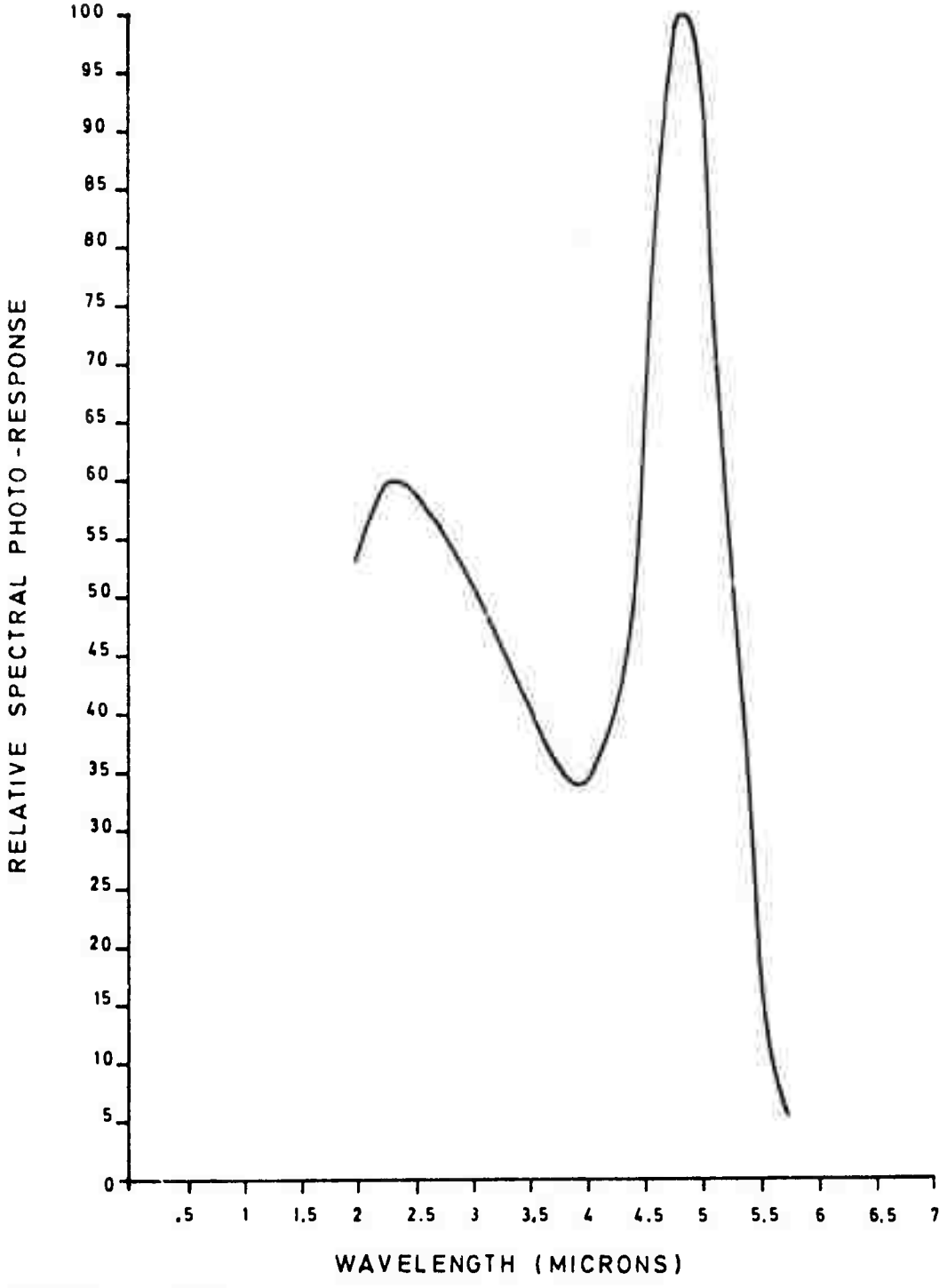

Figure 19. Relative spectral photoresponse of a p-type PbO_xS_{1-x} film.

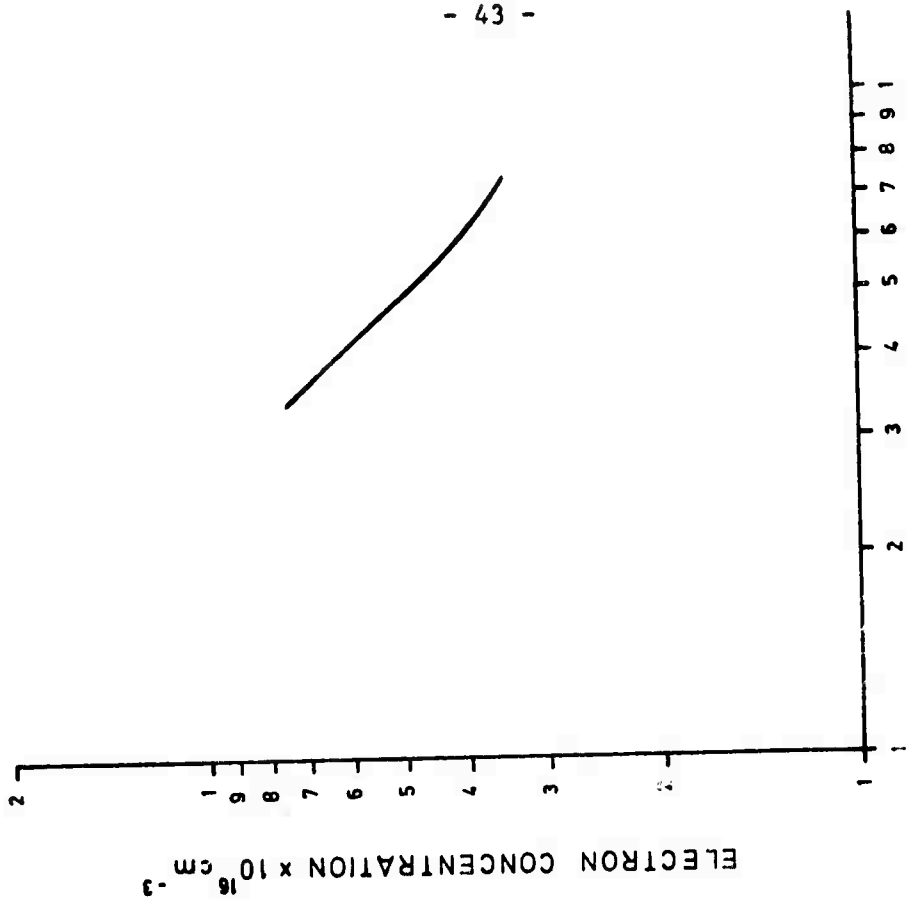

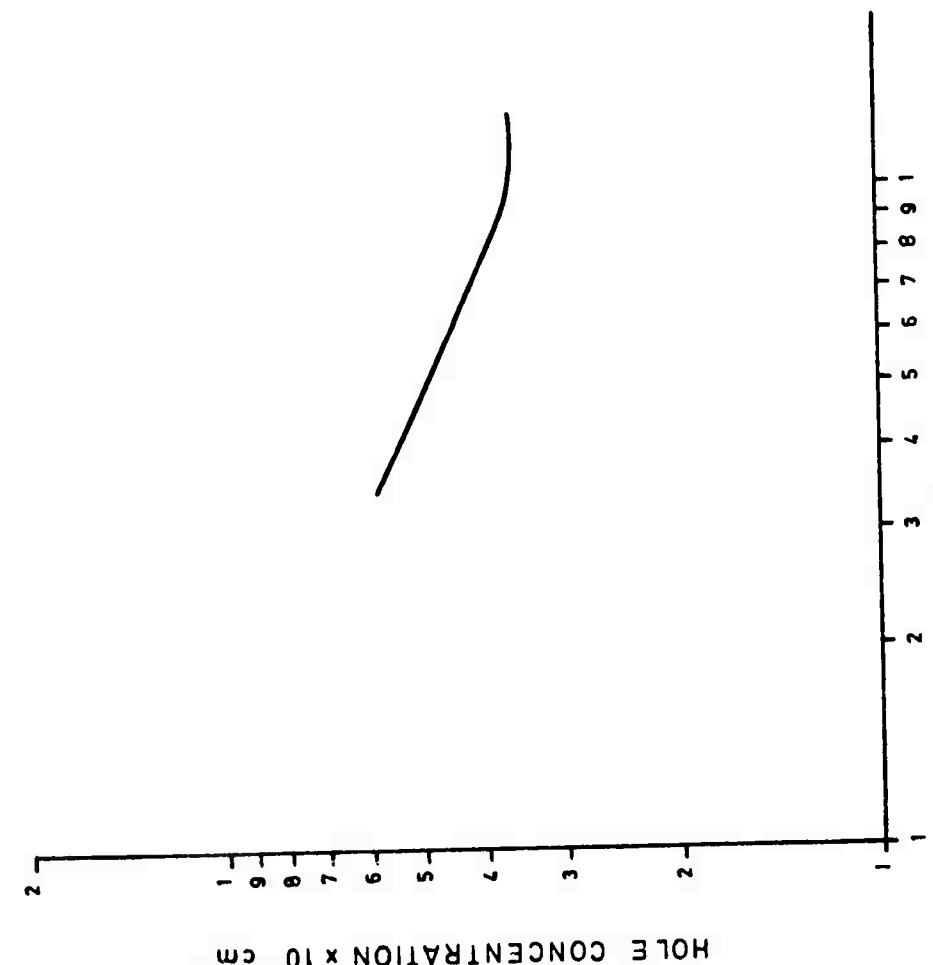

Figure 20. Temperature dependence of carrier concentration of n- and p-type PbO_xS_{1-x} films.

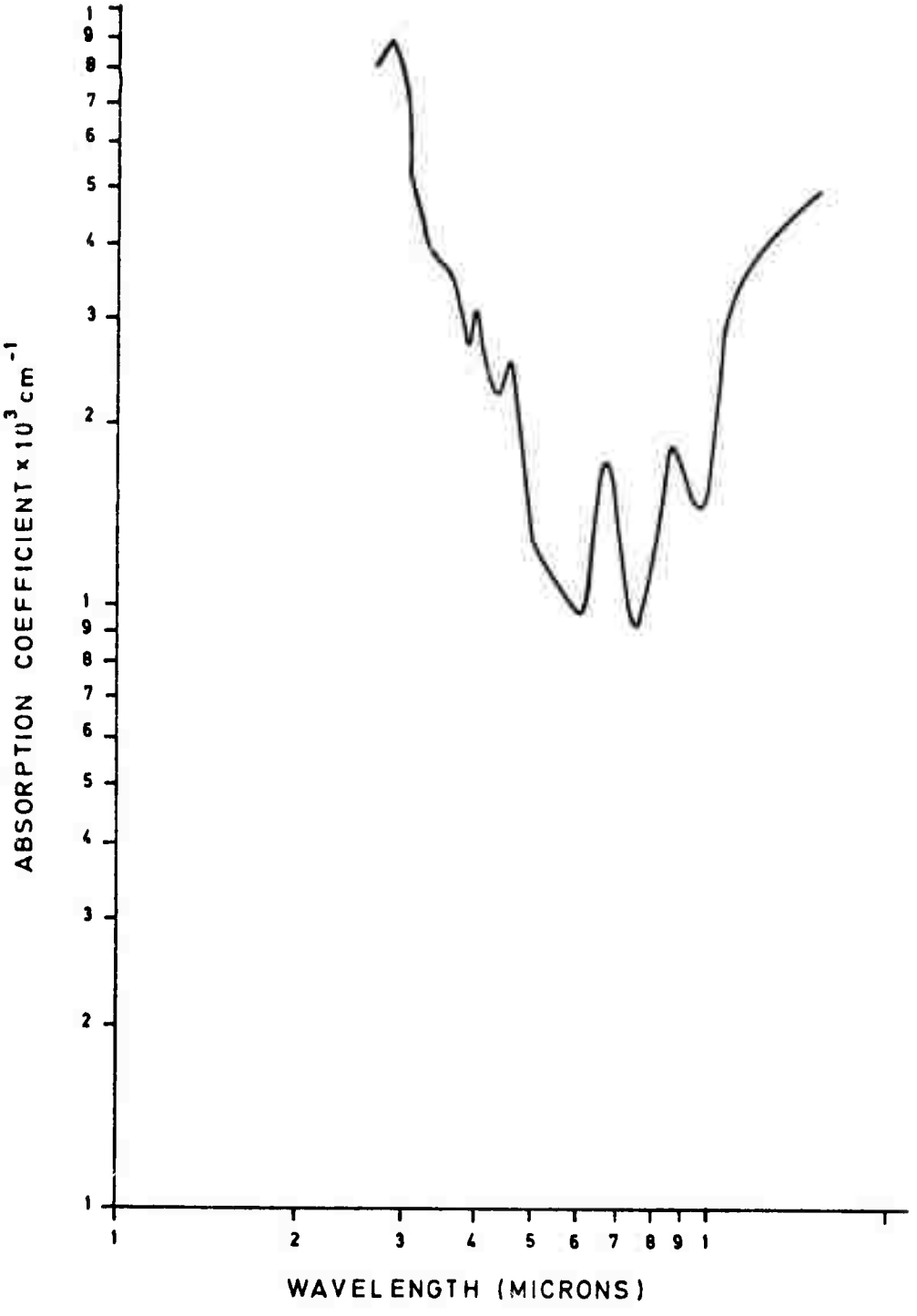

Figure 21. Absorption coefficient as a function of wavelength for a p-type PbO_xS_{1-x} film.

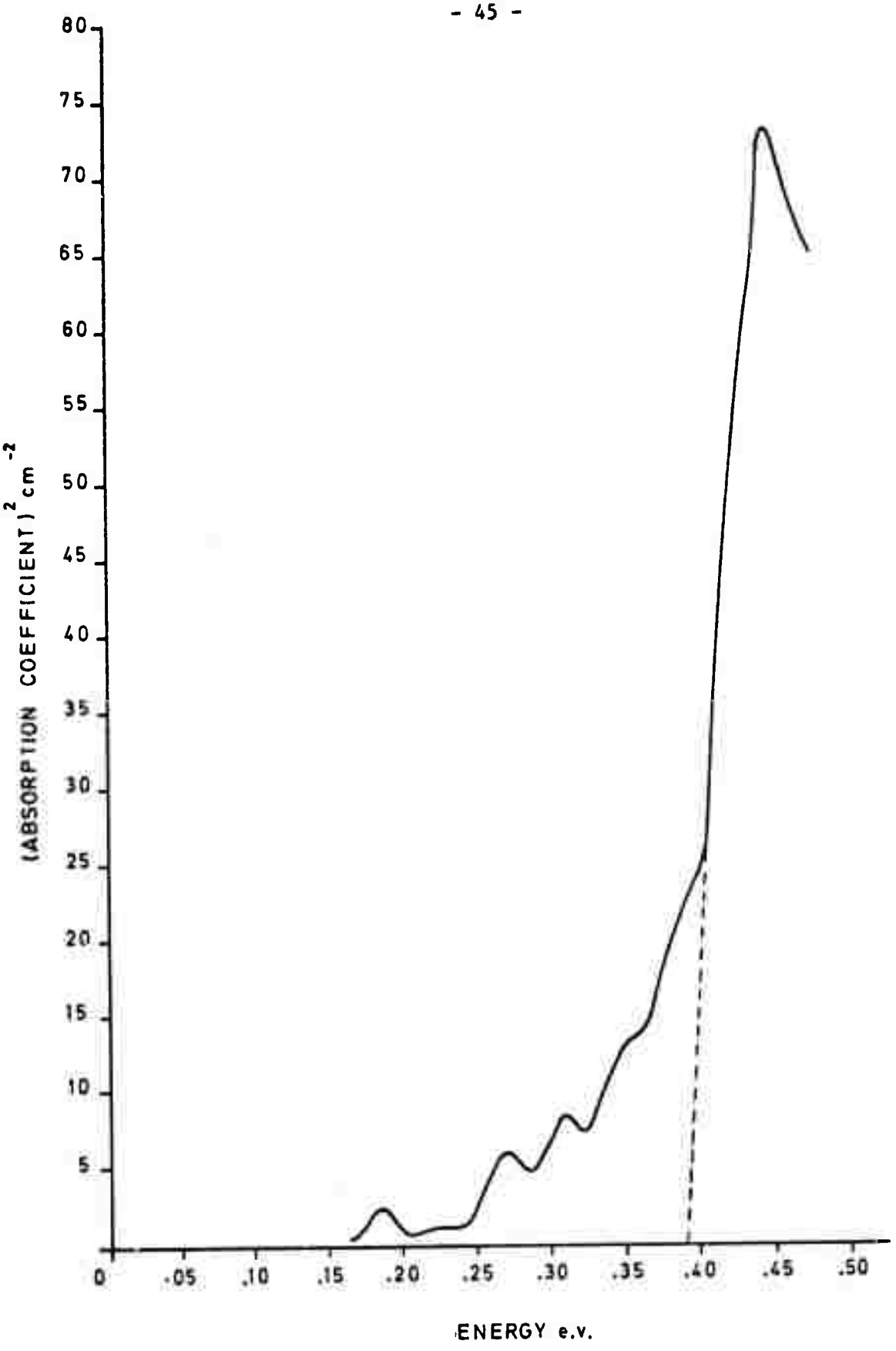

Figure 22. Square of absorption coefficient as a function of energy for a p-type PbO_xS_{1-x} film.